Synthesis and characterization of aryl substituted *bis*(2-pyridyl)amines and their copper olefin complexes: Investigation of remote steric control over olefin binding†

John J. Allen, Christopher E. Hamilton and Andrew R. Barron*

Received 5th June 2010, Accepted 14th July 2010
DOI: 10.1039/c0dt00608d

The aryl-functionalized pyridylamine 2-^{i}PrC$_6$H$_4$N(H)py (**1**) and bis(2-pyridyl)amines of the type ArN(py)$_2$ for Ar = Mes (**2**), 2,6-Et$_2$C$_6$H$_3$ (**3**), 2-^{i}PrC$_6$H$_4$ (**4**), 2,6-^{i}Pr$_2$C$_6$H$_3$ (**5**), and 1-naph (**6**), have been prepared by the palladium-catalyzed cross-coupling of substituted anilines with 2-bromopyridine, and have been characterized by ^{1}H and ^{13}C NMR NMR, FTIR, MS, and TGA. Complexes of these new N-aryl bis(2-pyridyl)amines have been prepared for the acid salts [H{ArN(py)$_2$}]BF$_4$ where Ar = Mes (**7**) and 2-^{i}PrC$_6$H$_4$ (**8**), and the dimeric bridged complexes [Cu{ArN(py)$_2$}(μ-X)(Y)]$_2$ where X/Y = Cl$^-$ and Ar = Ph (**9**), 2-^{i}PrC$_6$H$_4$ (**10**), and 1-naph (**11**), in addition to X = OH$^-$, Y = H$_2$O and Ar = Mes (**12**). The olefin complexes [Cu(Ar-dpa)(styrene)]BF$_4$ for Ar = Ph (**13**), Mes (**14**), 2-^{i}PrC$_6$H$_4$ (**15**), and 1-naph (**16**), in addition to the norborylene complexes of Ar = Mes (**17**) and 2-^{i}PrC$_6$H$_4$ (**18**) have been prepared and characterized by ^{1}H and ^{13}C NMR, FTIR, and TGA. The crystal structures have been determined for compounds **1–17**. Secondary amine **1** crystallizes in hydrogen-bonded head-to-tail dimers, while the N-aryl bis(2-pyridyl)amines **2–6** crystallize in a three-bladed propellar conformation, having nearly planar geometries about the amine nitrogen. The geometry about copper centers in the dimeric complexes **9–12** is distorted trigonal bypyramidal, with the axial positions occupied by one of the two pyridyl nitrogens and one of the bridging ligands (*i.e.*, Cl or OH). The copper atoms in each of the olefin complexes **13–17** are coordinated to the two pyridine nitrogen atoms and the appropriate olefin; consistent with a pseudo three-coordinate Cu(I) cation. Distortion of pyridyl ring geometries about the copper centers, and concomitant bending of the aryl groups away from the Cu···N(amine) vectors were found to correlate with the steric bulk of the aryl group present in both dimeric and olefin complexes. Such distortion is also observed to a lesser extent in the acid salts as well. The ^{1}H and ^{13}C NMR spectra of [Cu(Ar-dpa)(olefin)]BF$_4$ exhibit an upfield shift in the olefin signal as compared to free olefin. A good correlation exists between the ^{1}H and ^{13}C NMR $\Delta\delta$ values and olefin dissociation temperatures, confirming that the shift of the olefin NMR resonances upon coordination is associated with the binding strength of the complex.

Introduction

The control over the selective binding of olefins to a metal center has the potential as a simple route to overcoming the inherent difficulty in the separation of different olefins with near identical boiling points.[1,2] To this end, various complexing reagents have been described,[3] where the function of the complexing agent is to coordinate the olefin under one condition, and liberate it under another (eqn (1)).[4]

$$L_nM + R_2C{=}CR_2 \underset{\Delta}{\overset{rt}{\rightleftharpoons}} L_nM\text{-}\begin{Vmatrix} CR_2 \\ CR_2 \end{Vmatrix} \quad (1)$$

In designing a suitable coordination system for olefins, several groups have based the system on a biological model for ethylene complexation.[5,6] These studies have also demonstrated that stable Cu···olefin interactions can be achieved using multidentate, electron rich N-donor ligands.[7,8,9] The class of ligand most commonly used is the neutral N-donor heterocyclic compounds, including *bis*(pyrazolyl)methanes,[10] dipyridylamine,[11,12] phenanthroline,[13] and bipyridines.[14] Of all these studies, it is the report by Thompson and Whitney that has formed the basis for our studies. They showed that stable copper complexes with ethylene are formed with the chelate ligand *bis*(2-pyridyl)amine (Hdpa).

We have shown that the *bis*(2-pyridyl)amine ligand (**I**, where Ar = H) allows for the isolation and structural characterization of a wide range of ionic copper···olefin complexes.[15] We have observed that a twisting of the olefin out of the plane of the H-dpa ligand and a related folding of the H-dpa ligand provide relief of inter-ligand/intra-molecular steric strain for terminal and *cis*-olefins. Using ^{1}H and ^{13}C NMR we showed that there is a significant

Department of Chemistry, Rice University, Houston, Texas, 77005, USA. E-mail: arb@rice.edu

† Electronic supplementary information (ESI) available: IR and ^{13}C NMR spectral data. Thermal ellipsoid plots of the second unique molecule present in the asymmetric unit **3–5**, **14**, and **16** (including structural disorder for **4**), as well as comparisons between conformers for **3–5**, and **14**. Structural disorders for BF$_4^-$ in **7**, **8**, and **12–15**, and PF$_6^-$ in **17**. Highlighted intermolecular interactions present in **9**, **11–13**, and **17**. CCDC reference numbers 720342 (**1**), 720335 (**2**), 720338 (**3**), 720340 (**4**), 720339 (**5**), 720337 (**6**), 720347 (**7**), 735399 (**8**), 720344 (**9**), 733833 (**10**), 720343 (**11**), 720346 (**12**), 724010 (**13**), 724009 (**14**), 740151 (**15**), 743482 (**16**), and 728875 (**17**). For ESI and crystallographic data in CIF or other electronic format see DOI: 10.1039/c0dt00608d

difference in binding between a terminal and internal olefin, but there is much less preference between binding for different internal olefins. There is also a modest difference between the *cis* and *trans* isomers of the same olefin. These results suggested that while differential complexation of *cis* and *trans* isomers is possible using a H-dpa type ligand, separation of different internal olefins by their C=C position will not be possible. However, the use of pre-folded *bis*(2-pyridyl)amine ligands should allow for differentiation in coordination of olefin isomers.

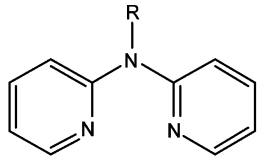

Ar = H, C_6H_5 (Ph), 2,4,6-$Me_3C_6H_2$ (Mes), 2,6-$Et_2C_6H_3$, 2-$^{i}PrC_6H_4$, 2,6-$^{i}Pr_2C_6H_3$, $C_{10}H_7$ (Naph)

(I)

During a study of the consequences of increased steric effects of quinolyl instead of pyridyl (*i.e.*, **II**[16] and **III**[17]) we have observed that the presence of a sterically hindered aryl group on the amine nitrogen results in a distortion about the amine nitrogen. Furthermore, molecular mechanics calculations on aryl substituted *bis*(2-pyridyl)amine ligands (**I**) suggest that the presence of the aryl substituent results in a folding of the *bis*(2-pyridyl)amine unit. Based upon this initial data we have proposed that steric substitution remotely from the metal could have an effect on the binding of an olefin to copper.

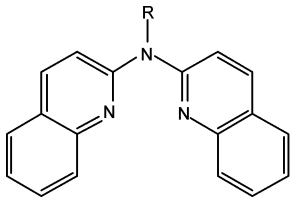

(II)

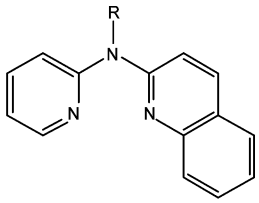

(III)

Herein we report the synthesis and structural characterization of a range of aryl substituted *bis*(2-pyridyl)amines (**I**), along with their copper complexes in order to determine how the steric bulk of the aryl substituent effects the geometry of the ligand. In addition, we report the affect of remote steric substitution on the binding of an olefin to copper.

Results and discussion

The direct reaction of an aniline with 2-bromopyridine yields the appropriate mono-pyridyl amine derivatives, *i.e.*, ArN(H)py, see Scheme 1. We have found that in order to prepare the associated dipyridyl amine derivatives, $ArN(py)_2$ (hereafter referred to as Ar-dpa), it is better to isolate the mono-pyridyl amine and react with additional 2-bromopyridine in the presence of a catalyst, see Scheme 1 and Experimental. Using these methods we have prepared the new pyridyl amine compounds, (2-$^{i}PrC_6H_5$)N(H)py (**1**), and Ar-dpa, where Ar = Mes (**2**), 2,6-$Et_2C_6H_3$ (**3**), 2-$^{i}PrC_6H_5$ (**4**), 2,6-$^{i}Pr_2C_6H_3$ (**5**), and naphthyl (**6**).

Compounds **1–6** have been characterized by NMR and IR spectroscopy, as well as mass spectrometry. The molecular structures for compounds **1–6** have been determined by single crystal X-ray diffraction. Selected bond lengths and angles can be found

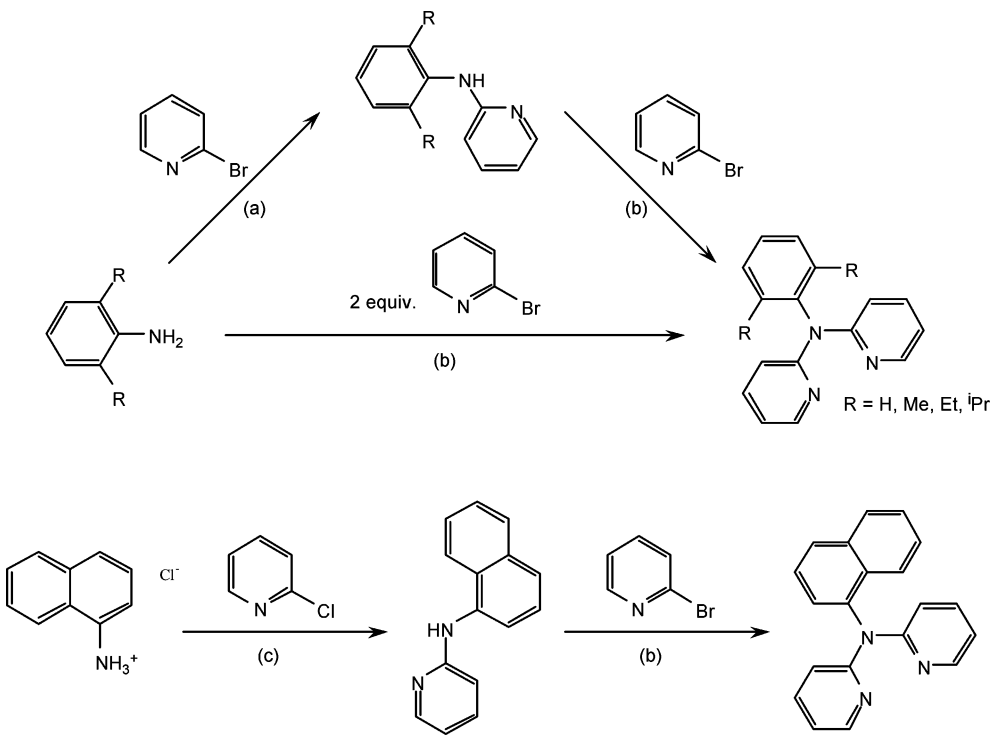

Scheme 1 Synthesis routes to Ar–dpa. (a) neat, reflux 2 h, (b) NaO^{t}Bu, Pd cat., toluene 90 °C, and (c) neat, 180 °C, 2 h.

Table 1 Selected bond lengths (Å) and angles (°) for compound **1**[a]

N(1)–C(1)	1.363(2)	N(1)–C(6)	1.419(2)
N(1)···N(2′)	2.995(2)		
N(1)–H(1a···N(2′)	173(2)	θAr	125.5(1)
χAr	85.4(2)	φAr	66.07(9)

[a] θ-bond angle Cpy–N–Ci; χ-torsion Npy–Cpy–Ci–(C N^{-1})I; φ-mean-plane angle from py ring.

in Tables 1 and 2. Details of data collection and structure solution and refinement are outlined in the Experimental section.

The molecular structure of the secondary aromatic amine compound **1** is shown in Fig. 1, selected bond lengths and angles are given in Table 1. Bond distances and angles measured between the amine nitrogen, N(1), and its substituent carbon atoms are within the ranges of those reported for ArN(H)py (Ar = Mes, 2,6-$Et_2C_6H_3$, 2,6-$^iPr_2C_6H_3$, and napthyl) [N–Cpy = 1.355(3)–1.370(6) Å; N–CAr = 1.415(6)–1.435(3) Å; Cpy–N–CAr = 122.4(1)–126.6(4)°].[18-24] As is typical for compounds of the type ArN(H)py, compound **1** crystallizes in the hydrogen-bonded head-to tail dimer, and the N–H···N interaction [N(1)···N(2′) = 2.995(2) Å] is comparable to those previously reported for analogous compounds [2.929(6) – 3.041(2) Å]. However, the presence of the bulky isopropyl group prevents any π–π stacking similar to that seen in homologous compounds.

The molecular structures for compounds **2–6** are shown in Fig. 2–6, while selected bond lengths and angles can be found in Table 2. Compounds **3–5** crystallize with two independent molecules in the asymmetric unit, and the atom numbering schemes for the second molecule of each are given in Fig. S1, S3, and S5.† The most significant differences observed between the two conformers are the orientation of alkyl substituents on the phenyl rings, the degree of pitch between the planes of the rings, and C–N–C bond angles between rings (Table 2 and Fig. S2, S4, and S6†).

The N–C bond lengths and the bond angles between the amine nitrogen and the heterocycles in the compounds **2–6** [1.398(3)–1.416(4) Å and 123.2(3)–124.6(1)°, respectively] are within the ranges to previously reported aryl-substituted dipyridylamines [1.400(2)–1.435(3) Å, 118.8(1)–123.8(1)°],[25,26] as well as N-alkyl pyridyl- and quinolyl-amines [1.378(4)–1.415(4) Å, 123.7(3)°].[27,28]

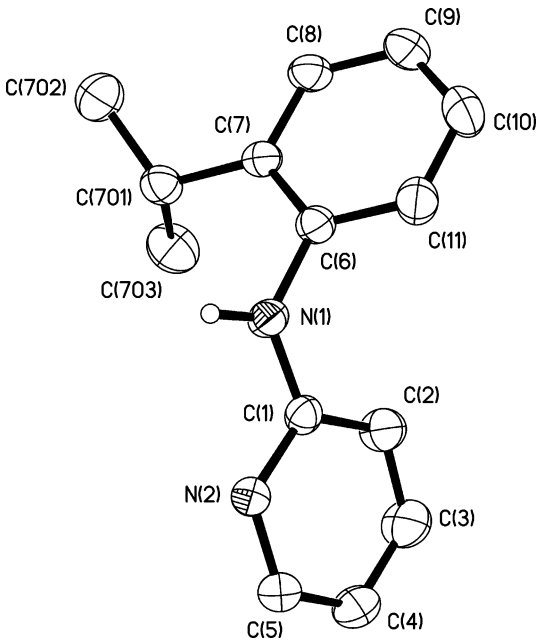

Fig. 1 Molecular structure of compound **1**. Thermal ellipsoids are shown at the 30% level, and hydrogen atoms attached to carbon are omitted for clarity.

The N–C bond lengths [1.438(5)–1.454(3) Å] and the angles between the tertiary amine nitrogen and the aryl substituent [116.4(3)–120.4(3)°] also seem to match well with similar compounds [1.415(3)–1.463(4) Å and 117.2(1)–121.3(2)°, respectively].

The geometry about N(1) in compounds **2–6** is essentially planar (∑C–N–C = 359.3 – 360°); consequently the pyridyl and aryl rings are forced to twist out of plane due to the steric bulk of the *ortho*-substituents. Thus, as proposed, the presence of the aryl's substituents forces the pyridyl rings out of plane from the NC_3 core. Interestingly, the trend is the opposite of what may be expected, *i.e.*, the greater the steric bulk of the *ortho*-substituents the more co-planar the pyridyl rings. This may be seen from a consideration of either the N(2)–C(1)···C(6)–N(3) torsion angle or the angle between the mean plane of each pyridyl ring (MPLN[py–py′]) for compounds **2** (R = Me), **3** (R = Et), and **5** (R = ^{i}Pr), see Table 2. In part, this may be explained by a greater twisting of the aryl ring with respect to the amines's NC_3 core with

Table 2 Selected bond lengths (Å) and angles (°) for Ar–dpa

Compound	**2**	**3**[a]	**4**[a]	**5**[a]	**6**
N(1)–C(1)	1.398(3)	1.402(5), 1.402(5)	1.403(4), 1.395(4)	1.405(3), 1.405(3)	1.411(1)
N(1)–C(6)	1.411(3)	1.403(5), 1.413(5)	1.411(4), 1.416(4)	1.387(3), 1.400(3)	1.410(1)
N(1)–C(11)	1.439(3)	1.442(5), 1.438(5)	1.445(5), 1.453(4)	1.454(3), 1.451(3)	1.442(1)
C(1)–N(1)–(6)	124.0(2)	123.4(3), 123.2(3)	123.7(3), 124.6(3)	124.0(1), 124.5(2)	124.6(1)
C(1)–N(1)–C(11)	118.3(2)	117.8(3), 120.4(3)	118.2(3), 118.7(3)	117.5(2), 117.3(1)	117.0(1)
C(6)–N(1)–C(11)	117.6(1)	118.6(3), 116.4(3)	117.8(3), 116.6(3)	117.8(1), 118.0(1)	117.9(1)
N(2)–C(1)–C(6)–N(3)	119.1(3)	119.1(4), 126.9(5)	124.1(5), 127.8(5)	120.3(3), 128.9(3)	137.2(1)
N(2)–C(1)–N(1)–C(11)	151.4(2)	21.8(5), 15.3(6)	156.1(4), 159.3(4)	22.3(3), 23.6(3)	155.7(1)
N(3)–C(6)–N(1)–C(11)	24.1(4)	149.5(5), 145.6(4)	22.0(5), 24.3(4)	153.8(2), 162.0(2)	17.5(1)
MPLN[py–py′]	48.7(1)	47.5(2), 46.5(2)	43.3(2), 41.8(2)	46.4(1), 40.7(1)	42.17(7)
MPLN[py–Ar]	82.0(1)	87.3(2), 82.1(2)	85.8(2), 84.9(2)	88.9(1), 85.1(1)	84.02(7)
MPLN[py′–Ar]	81.1(1)	87.3(2), 86.5(2)	88.8(2), 85.4(2)	81.7(1), 79.7(1)	69.49(7)

[a] Two crystallographically independent molecules in the asymmetric unit. The atom numbering scheme for the second molecule is given in Fig. S1, S3, and S5.†

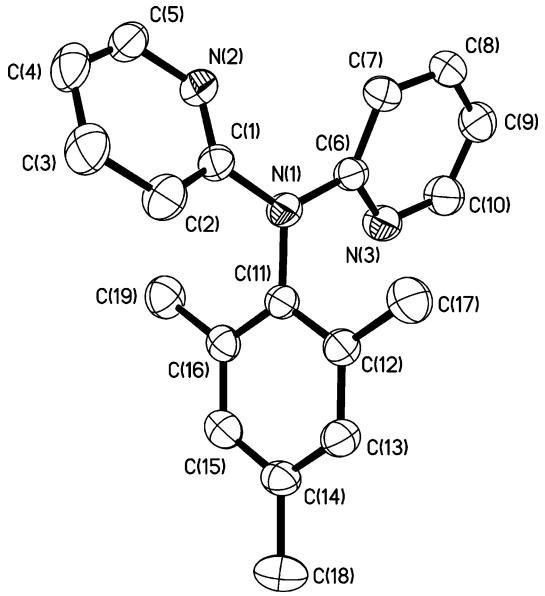

Fig. 2 Molecular structure of compound **2**. Thermal ellipsoids are shown at the 30% level, and all hydrogen atoms are omitted for clarity.

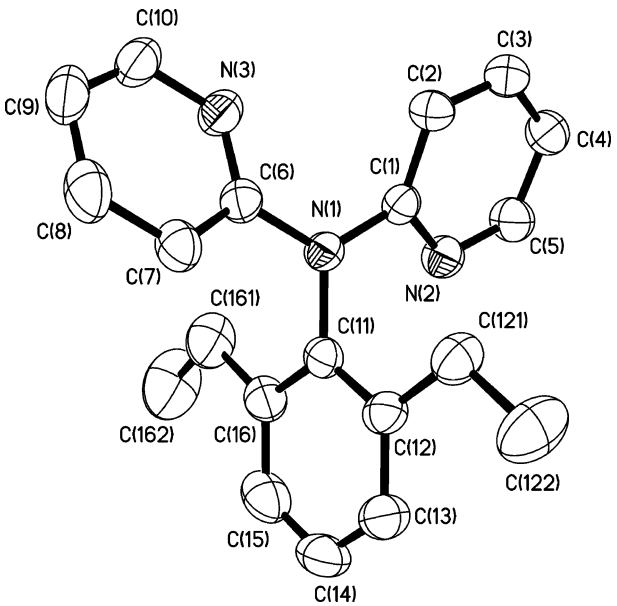

Fig. 3 Molecular structure of one of the two crystallographically independent molecules of **3**. Thermal ellipsoids are shown at the 30% level, and all hydrogen atoms are omitted for clarity.

larger substituents. As may be seen from Table 2, the pyridyl rings appear more coplanar for asymmetrically substituted aryl groups.

A plot of N(1)–C(11) bond distance (also an indirect measure of the twist of the aryl ring) *versus* the angle between the mean plane of each pyridyl ring (MPLN[py–py′]) for compounds **2–6**, as well as the previously reported analogs shows a distinct trend (Fig. 7a). The inter-pyridyl angle [C(1)–N(1)–C(6)] is also dependent on the N(1)–C(11) distance (Fig. 7b). However, a closer consideration of the *ortho*-*versus para*-substitution suggests that electronic factors also come into play. Specifically, *ortho*-substituents result in longer bond lengths and larger bond angles.

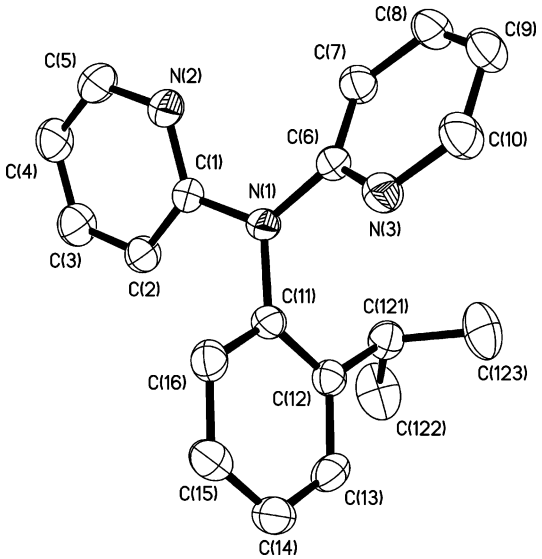

Fig. 4 Molecular structure of one of the two crystallographically independent molecules of compound **4**. Thermal ellipsoids are shown at the 30% level, and all hydrogen atoms are omitted for clarity.

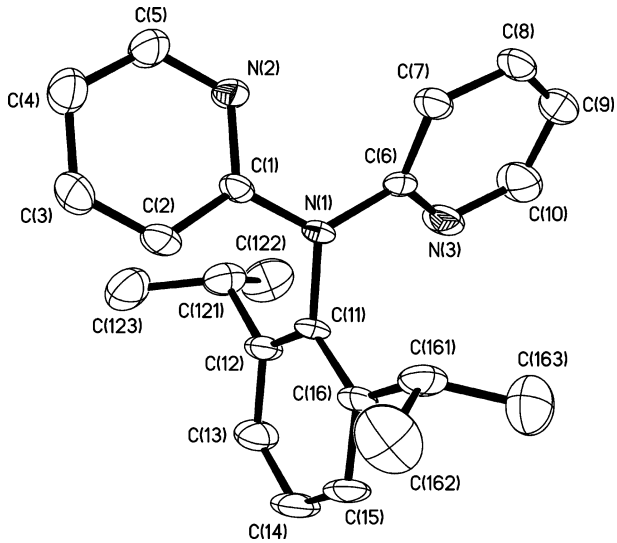

Fig. 5 Molecular structure of one of the two crystallographically independent molecules of compound **5**. Thermal ellipsoids are shown at the 30% level, and all hydrogen atoms are omitted for clarity.

Based upon the forgoing, the presence of *ortho*-substitution in the uncomplexed Ar-dpa compounds results in a significant distortion of the coordination around the amine nitrogen and twisting of the two pyridyl rings with respect to each other.

Acid confinement of the conformation of the pyridyl rings in Ar-dpa

Based upon the structural trends of compounds **2–6**, it is clear that the steric bulk of the aryl substituents has a controlling influence on the orientation of the pyridyl rings. In the free compounds this influence results in the twisting of the pyridyl rings with regard to each other, and their splaying out [*i.e.*, increased C(1)–N(1)–C(6) angle] to relieve the steric strain imposed by the aryl's *ortho*-substituents. However, in a coordination complex the pyridyl nitrogen atoms are held by the geometry of the complex,

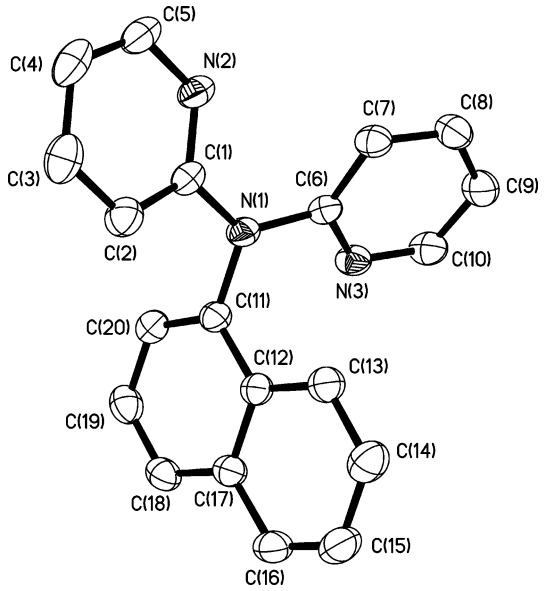

Fig. 6 Molecular structure of compound **6**. Thermal ellipsoids are shown at the 30% level, and all hydrogen atoms are omitted for clarity.

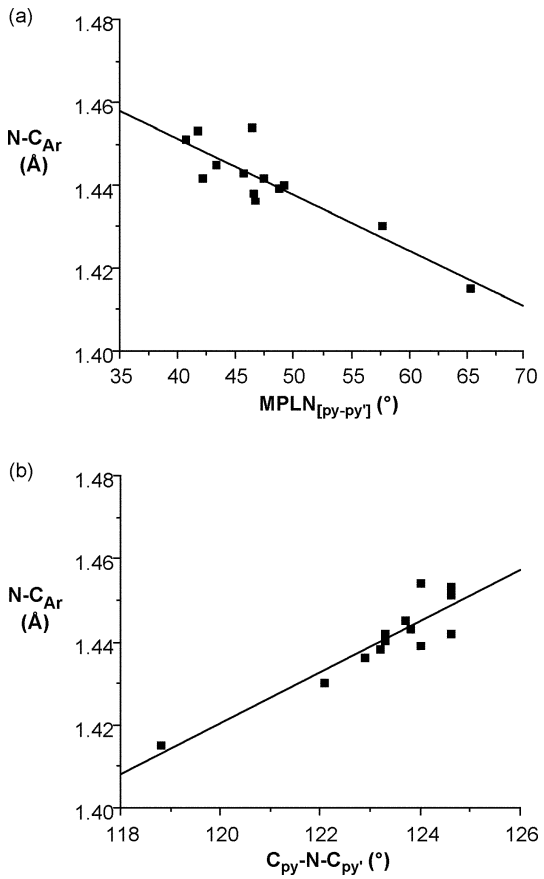

Fig. 7 Plot of the N–CAr bond lengths *versus* (a) the mean-plane-difference between pyridyl rings ($R_2 = 0.793$) and (b) Cpy–N–Cpy′ bond angle ($R = 0.828$) for compounds **2–6**, as well as previously reported Ar–dpa derivatives.

and thus a different distortion will be required to release the steric strain. We have previously reported that the protonation of the N-(2-pyridyl)-*N*-(2-quinolyl)amine, PhN(py)quin, results in confinement in the orientation of the pyridyl and quinolyl rings in the isolated complex, [PhN(py)(H-quin)]BF_4.[17] In order to ascertain the geometric effects of the aryl substituents in a simple complex we have structurally characterized the protonated derivatives. Protonation of $ArN(py)_2$ can be accomplished by the reaction of KBF_4 dissolved in dilute HCl (Experimental).[17] The molecular structures of **7** and **8**, which are the HBF_4 salts of compound **2** and **4**, respectively, are shown in Fig. 8 and Fig. 9. Selected bond lengths and angles are given in Table 3.

Table 3 Selected bond lengths (Å) and angles (°) for compounds **7** and **8**

	7	**8**
N(1)–C(1)	1.394(3)	1.382(3)
N(1)–C(6)	1.417(3)	1.403(3)
N(1)–C(11)	1.453(3)	1.449(3)
N(2)···H	1.04(3)	1.18(3)
N(3)···H	1.61(3)	1.51(3)
F···H	2.40(3)	2.28(3)
C(1)–N(1)–C(6)	124.6(1)	125.4(2)
C(1)–N(1)–C(11)	117.1(1)	116.9(2)
C(6)–N(1)–C(11)	118.1(1)	117.7(2)
N(2)–H···F	120(2)	114(2)
MPLN[py–py′]	5.0(1)	1.7(1)
MPLN[py–Ar]	83.3(1)	89.5(1)
MPLN[py′–Ar]	81.3(1)	89.4(1)

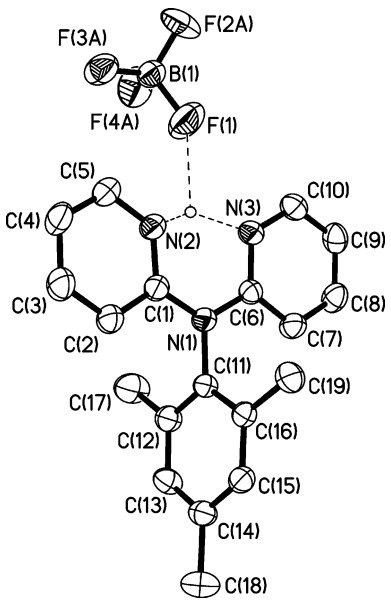

Fig. 8 Molecular structure of [(Mes–dpa)H]BF_4 (**7**). Thermal ellipsoids are shown at the 30% level, and hydrogen atoms attached to carbon are omitted for clarity.

The pyridyl nitrogens in compounds **7** and **8** are found to coordinate the proton in an asymmetric fashion (Table 3). This degree of asymmetry is not observed in the structurally similar $HClO_4$ and HBr salts [1.362(6) and 1.362(6) Å; 1.33 and 1.40 Å],[29] or the [(H-dpa)H]$CoCl_4$ complex [1.33(3) and 1.36(3) Å].[30] The asymmetry is more pronounced for the mesityl derivative (**7**) than the 2-$^{i}PrC_6H_4$ compound (**8**).

The N–C distances about the amine nitrogen in compounds **7** and **8** are similar to those observed in the free ligands. Consideration of the fold angle, *i.e.*, the mean-plane-angle difference between

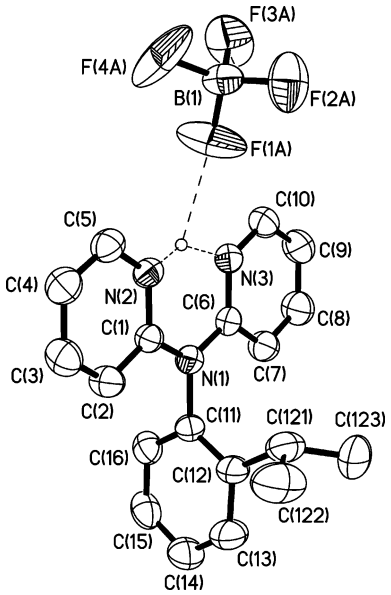

Fig. 9 Molecular structure of $[(2\text{-}^{i}Pr\text{–}C_6H_4\text{–}dpa)H]BF_4$ (**8**). Thermal ellipsoids are shown at the 30% level, and hydrogen atoms attached to carbon are omitted for clarity.

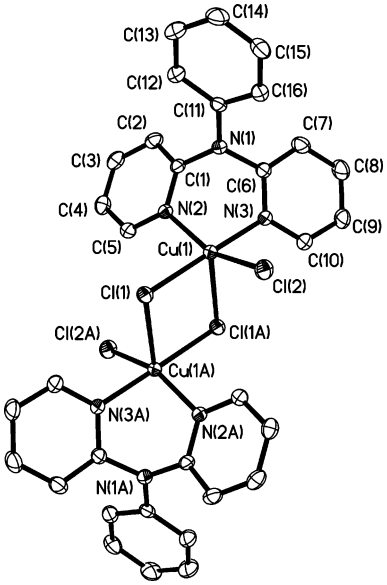

Fig. 10 Molecular structure of the $[Cu(Ph\text{–}dpa)(Cl)(\mu\text{-}Cl)]_2$ (**9**) dimer. Thermal ellipsoids are shown at the 30% level, and all hydrogen atoms are omitted for clarity.

pyridyl rings [5.0(1) and 1.7(1)°, respectively], and the N–C–C–N torsion angle across the amine-bound carbons [4.9(2) and 1.3(2)°, respectively], reveals that, in contrast to the free ligands, the two heterocycles are almost coplanar in the complexes. However, as a result of the forcible co-planarity of the two pyridyl rings, there is a bending-up of the aryl group out of the di-pyridyl plane. The observed bending of the aryl group is found to be slightly greater for the mesityl derivative [8.0(8)° *versus* 4.9(6)°].

The presence of *ortho*-substitution in the complexed Ar-dpa compounds, in which the two pyridyl rings are constrained by a complexed atom, results in the bending-up of the aryl ring substituent out of the di-pyridyl plane with consequential folding of the two pyridyl into a "butterfly" conformation. In order to ascertain whether these distortions translate to metal derivatives we have structurally characterized simple dimeric copper complexes of Ar-dpa.

Copper(II) complexes of Ar–dpa

The copper complexes $[Cu(Ph\text{–}dpa)(Cl)(\mu\text{-}Cl)]_2$ (**9**), $[Cu(2\text{-}^{i}PrC_6H_4\text{–}dpa)(Cl)(\mu\text{-}Cl)]_2$ (**10**), and $[Cu(Nap\text{–}dpa)(Cl)(\mu\text{-}Cl)]_2\cdot(MeOH)_2$ (**11**) are prepared by the reaction of $[Cu(MeCN)_4]BF_4$ with the appropriate Ar–dpa in tetraethylelene glycol in the presence of dilute HCl. If the reaction is carried out using Mes–dpa (**2**) in the presence of water, the structurally related hydroxy derivative, $[Cu(Mes\text{–}dpa)(H_2O)(\mu\text{-}OH)]_2[BF_4]_2\cdot(MeOH)_2$, (**12**) is isolated. Despite the difference in ligation and charge, compound **12** is isolobal with compounds **9–11**.

The molecular structures of compounds **9–11** are shown in Fig. 10–12; selected bond lengths and angles are given in Table 4. The structure of the cation, $[Cu(Mes\text{–}dpa)(H2O)(\mu\text{-}OH)]_2^{+}$, is shown in Fig. 13, with selected bond lengths and angles given in Table 5. Compounds **9**, **11**, and **12** crystallize with only half of the molecule in the asymmetric unit of the unit cell. In each case,

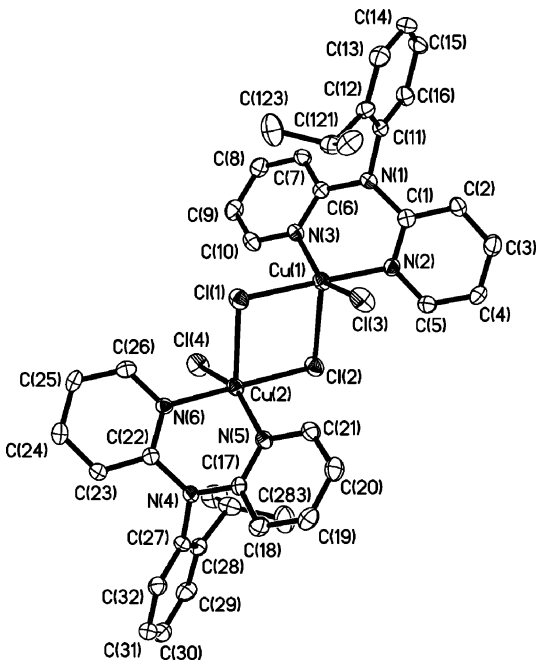

Fig. 11 Molecular structure of the $[Cu(2\text{-}^{i}PrC_6H_4\text{–}dpa)(Cl)(\mu\text{-}Cl)]_2$ (**10**) dimer. Thermal ellipsoids are shown at the 30% level, and all hydrogen atoms are omitted for clarity.

the second half of the molecule is symmetry related through an inversion center.

The coordination geometry about the copper centers in compounds **9–12** is a distorted trigonal bipyramid, with the axial positions occupied by one of the two pyridyl nitrogens and one of the bridging ligands (*i.e.*, Cl or OH), with the *trans*-angle ranging from 171.8(1)–178.2(1)° (Tables 4 and 5). The trigonal bipyramidal coordination spheres observed in these bridged dimers is common in other structurally related

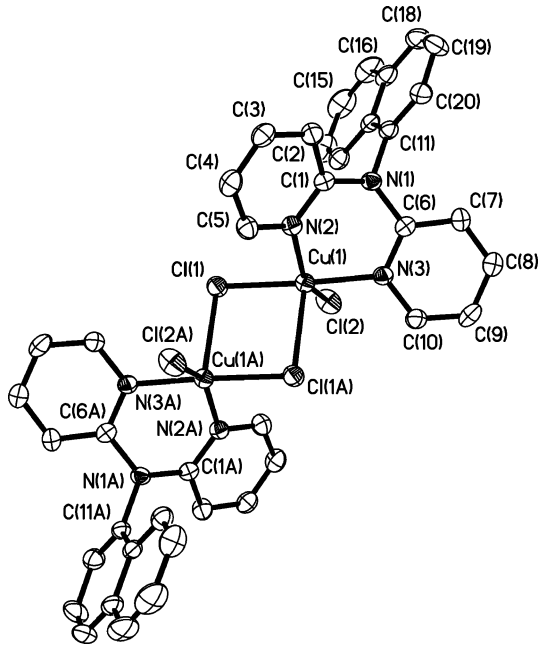

Fig. 12 Molecular structure of the $[Cu(Naph–dpa)(Cl)(\mu\text{-}Cl)]_2$ (**11**) dimer. Thermal ellipsoids are shown at the 30% level, and all hydrogen atoms are omitted for clarity.

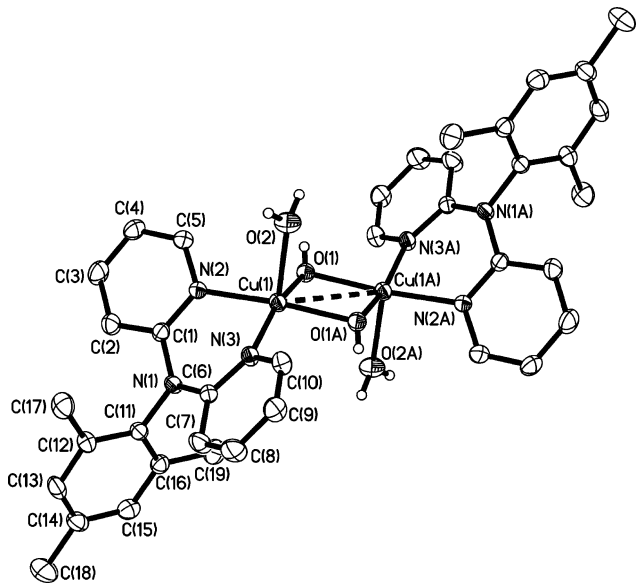

Fig. 13 Molecular structure of the $[Cu(Mes-dpa)(H_2O)(\mu\text{-}OH)]_2^{2+}$ cation (**12**). Thermal ellipsoids are shown at the 30% level, and hydrogen atoms attached to carbon are omitted for clarity.

Table 4 Selected bond lengths (Å) and angles (°) for compounds **9–11**

Compound	**9**[a]	**10**	**11**[a]
Cu(1)–Cl(1)	2.2755(6)	2.261(1)	2.296(2)
Cu(1)–Cl(1A)	2.7299(7)	2.698(1)[b]	2.596(2)
Cu(2)–Cl(1)		2.264(1)	
Cu(2)–Cl(2)		2.683(1)	
Cu(1)–Cl(2)	2.2547(9)	2.286(1)[c]	2.285(2)
Cu(2)–Cl(4)		2.285(1)	
Cu(1)–N(2)	2.025(1)	2.013(4)	2.020(6)
Cu(1)–N(3)	2.030(1)	2.018(4)	1.998(6)
Cu(2)–N(5)		2.016(4)	
Cu(2)–N(6)		2.028(4)	
N(1)–C(1)	1.421(2)	1.399(6)	1.415(9)
N(4)–C(17)		1.417(6)	
N(1)–C(6)	1.421(3)	1.412(7)	1.404(8)
N(4)–C(22)		1.403(6)	
N(1)–C(11)	1.416(3)	1.450(7)	1.466(8)
N(4)–C(27)		1.454(6)	
Cu(1)···Cu(1A)	3.6728(8)	3.594(1)[d]	3.513(1)
Cl(1)–Cu(1)–Cl(1A)	86.03(2)	87.64(5)[e]	88.41(7)
Cl(1)–Cu(2)–Cl(2)		88.03(5)	
Cl(1)–Cu(1)–Cl(2)	93.45(3)	92.85(6)[f]	91.92(9)
Cl(2)–Cu(2)–Cl(4)		93.39(6)	
Cl(1)–Cu(1)–N(2)	92.01(5)	177.8(1)	92.4(1)
Cl(1)–Cu(1)–N(3)	176.18(5)	93.4(1)	177.2(1)
Cl(2)–Cu(2)–N(6)		178.2(1)	
Cl(1)–Cu(2)–N(5)		99.0(1)	
Cl(2)–Cu(1)–N(2)	156.14(5)	90.5(1)[g]	148.7(1)
Cl(2)–Cu(1)–N(3)	89.30(5)	97.5(1)[h]	88.6(1)
N(2)–Cu(1)–N(3)	86.52(6)	86.7(1)	85.7(2)
N(5)–Cu(2)–N(6)		85.6(1)	
Cu(1)–Cl(1)–Cu(1A)	93.97(2)	92.30(5)[i]	91.59(7)
C(1)–N(1)–C(6)	115.6(1)	122.4(4)	123.1(6)
C(17)–N(4)–C(22)		122.1(4)	
C(1)–N(1)–C(11)	121.1(1)	119.3(4)	118.4(5)
C(17)–N(4)–C(27)		118.6(4)	
C(22)–N(4)–C(27)	123.1(1)	118.1(4)	118.0(6)
		119.2(4)	

[a] Centrosymmetric structures. [b] Cu(1)–Cl(2). [c] Cu(1)–Cl(3). [d] Cu(1)–Cu(2). [e] Cl(1)–Cu(1)–Cl(2). [f] Cl(1)–Cu(1)–Cl(3). [g] Cl(3)–Cu(1)–N(2). [h] Cl(3)–Cu(1)–N(3). [i] Cu(1)–Cl(1)–Cu(2).

Table 5 Selected bond lengths (Å) and angles (°) for compound **12**

Cu(1)–N(2)	1.977(2)	Cu(1)–N(3)	1.987(2)
Cu(1)–O(1)	1.960(2)	Cu(1)–O(1a)	1.953(2)
Cu(1)–O(2)	2.223(3)	N(1)–C(1)	1.404(3)
N(1)–C(6)	1.407(3)	N(1)–C(11)	1.453(4)
Cu(1)···Cu(1a)	2.9666(9)		
N(2)–Cu(1)–N(3)	86.6(1)	N(2)–Cu(1)–O(1)	94.73(9)
N(2)–Cu(1)–O(1A)	171.8(1)	N(2)–Cu(1)–O(2)	95.6(1)
N(3)–Cu(1)–O(1)	162.4(1)	N(3)–Cu(1)–O(1A)	94.9(1)
N(3)–Cu(1)–O(2)	101.3(1)	O(1)–Cu(1)–O(1A)	81.39(9)
O(1)–Cu(1)–O(2)	96.0(1)	Cu(1)–O(1)–Cu(1a)	98.61(9)
C(1)–N(1)–C(6)	125.4(2)	C(1)–N(1)–C(11)	116.6(2)
C(6)–N(1)–C(11)	116.8(2)		

compounds $[Cu\{CH_2(py)_2\}(Cl)(\mu\text{-}Cl)]_2$,[31] $[Cu(o\text{-}phen)(Cl)(\mu\text{-}Cl)]_2$,[32] $[Cu(bipy)(Cl)(\mu\text{-}Cl)]_2$,[33] and $[Cu(o\text{-}phen)(H_2O)(\mu\text{-}OH)]_2NO_3$.[34]

The Cu–Cl distances between bridging and non-bridging chlorine atoms in **9–11** are with the ranges [2.255(3)–2.722(3) Å and 2.256(1)–2.272(3) Å] previously reported for similar compounds.[31–33] The Cu–O distances for the bridging hydroxo ligands [1.960(2) and 1.953(2) Å] are similar to those reported for the aforementioned *ortho*-phen complex [1.944(3) Å], the neutral β-diketiminato complex [1.914(1) and 1.923(1) Å],[35] the bipy/PhNHpy complex [1.94(1) and 1.96(1) Å],[36] and the bis(imidazolin-2-imine) complex [1.932(2) and 1.930(2) Å].[37] The Cu–O distance for the aquo ligand [2.223(3)] is also similar to those previously reported [2.035(4)–2.518(1) Å].[38,39] The observed Cu–(μ-O)–Cu(1A) angle in **12** is slightly larger than the corresponding angles in the chloride analogs, but much longer distances between bridging atoms in the latter result in significantly longer [3.513(1)–3.6728(8) Å] Cu···Cu distances than in **12** [2.9666(9) Å].

Overall, the $[Cu(X)(\mu\text{-}X)_2Cu(X)]$ core in compounds **9–12** is rigid and appears to be unaffected by the nature of the Ar–dpa

ligand. It is therefore useful to look at the distortions in the Ar-dpa ligands as a function of the steric bulk of the aryl substituents. As may be seen from Fig. 14, the bend of the N–CAr out of the plane of the two pyridyl rings is proportional to the folding along the Cu···N vector (*i.e.*, formation of a butterfly conformation). It is interesting to note that of the ligands studied, it is the phenyl derivative (compound **9**) that appears to have the greatest steric differentiation about the copper due to the remotely substituted aryl. Observation of Fig. 10–13, suggests that this is because of the almost eclipsed orientation of the phenyl with respect to the two pyridyl rings. Clearly, in solution this will be averaged due to free rotation about the N(1)–C(11) bond.

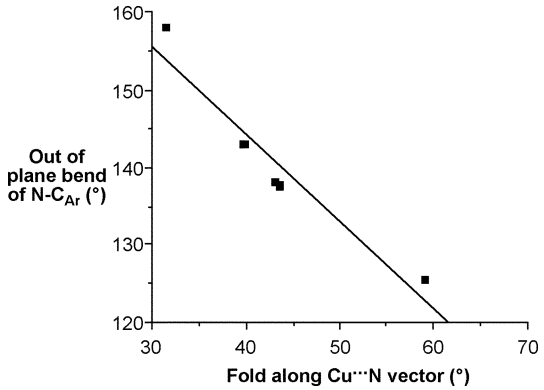

Fig. 14 Plot of the bend of the N–CAr out of the plane of the two pyridyl rings *versus* folding along the Cu···N vector for compounds **9–12** (R_2 = 0.928).

Based upon the forgoing, the presence of *ortho*-substitution in the uncomplexed Ar–dpa compounds results in a significant distortion of the coordination around the amine nitrogen and twisting of the two pyridyl rings with respect top each other. What this result does show is that the steric bulk of the substituents on the aryl ring in Ar–dpa does have a significant effect on the orientation and configuration of the two pyridyl rings, even when the pyridyl nitrogens are rigidly coordinated to a copper center.

Effect on olefin binding by the remote steric bulk of the Ar–dpa ligands

The reaction of $[Cu(MeCN)_4]BF_4$ with styrene in the presence of the appropriate Ar–dpa results in the formation of the olefin complex, $[Cu(Ar–dpa)(\eta^2\text{-styrene})]BF_4$ (eqn (2)) where Ar – Ph (**13**), Mes (**14**), (2-^{i}Pr)Ph (**15**), and naph (**16**). The analogous norbornylene derivatives, $[Cu(Ar–dpa)(\eta^2\text{-norbornylene})]X$, where Ar = Mes with X = PF_6 (**17**) and (2-^{i}Pr)Ph with X = BF_4 (**18**), were also prepared using Mes–dpa (**2**) and ^{i}Pr$_2$-dpa (**4**) as ligands, respectively.

$$[Cu(MeCN)_4]BF_4 + Ar–dpa + \text{styrene} \rightarrow [Cu(Ar–dpa)(\eta^2\text{-styrene})]BF_4 + 4\ MeCN \quad (2)$$

Compounds **13–18** are soluble in alcohols and show instability in air and have been characterized by ^{1}H and ^{13}C NMR, FT-IR, and TG/DTA. The crystal structures of compounds **13–17** have been determined.

The structure of the complex cation, $[Cu(Ar–dpa)(\eta^2\text{-styrene})]^+$, in compounds **13–16** are shown in Fig. 15–18. Selected bond lengths and angles are compared in Table 6 with those of

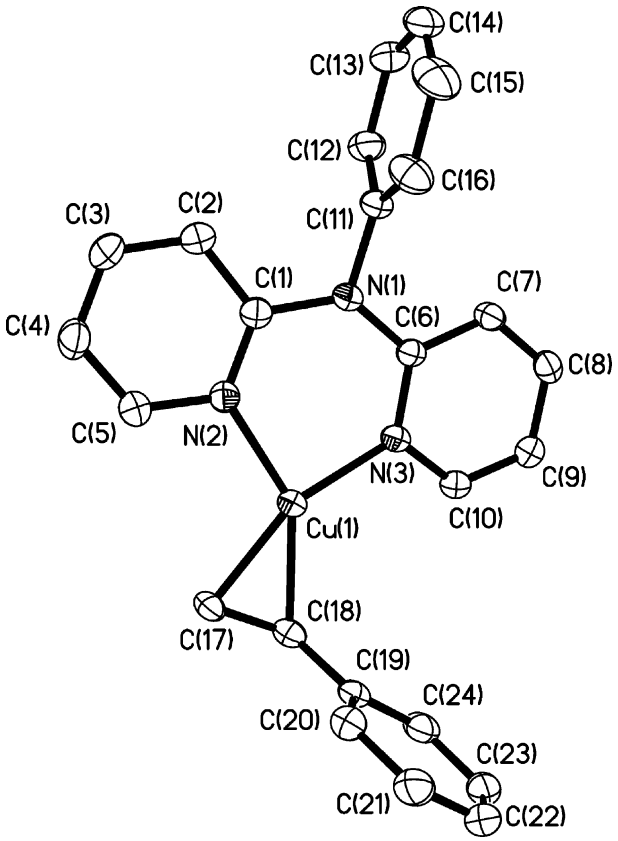

Fig. 15 Structure of the $[Cu(Ph–dpa)(\eta^2\text{-styrene})]^+$ cation in compound **13**. Thermal ellipsoids are shown at the 30% level, and hydrogen atoms attached to carbon are omitted for clarity.

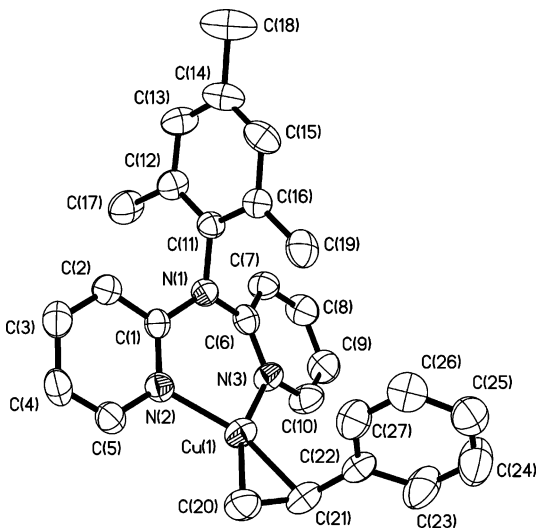

Fig. 16 Structure of the $[Cu(Mes-dpa)(\eta^2\text{-styrene})]^+$ cation in compound **14**. Thermal ellipsoids are shown at the 30% level, and hydrogen atoms attached to carbon are omitted for clarity.

$[Cu(H-dpa)(\eta^2\text{-styrene})]^+$ that we have previously reported.[15] Two independent molecules of compounds **14** and **16** are present in the asymmetric unit, and the numbering schemes for the second molecules are given in Fig. S15 and Fig. S19.† As with the other BF_4^- salts, the anion is disordered in the solid state for compounds **13–15** (see Experimental and Fig. S13, S17, and S18†).

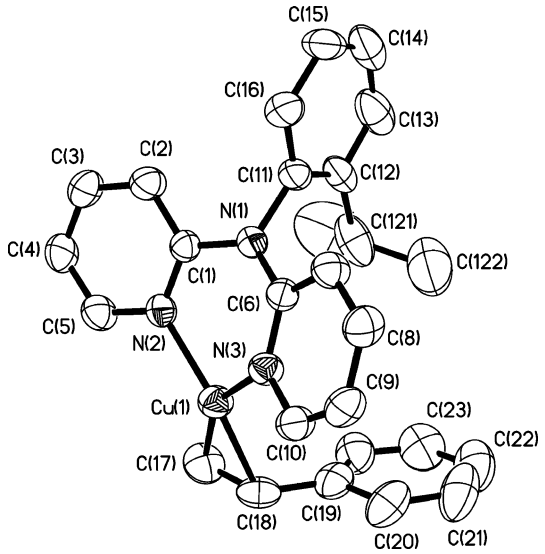

Fig. 17 Structure of the $[Cu(2\text{-}^{i}PrC_6H_4\text{-dpa})(\eta^2\text{-styrene})]^+$ cation in compound **15**. Thermal ellipsoids are shown at the 30% level, and hydrogen atoms attached to carbon are omitted for clarity.

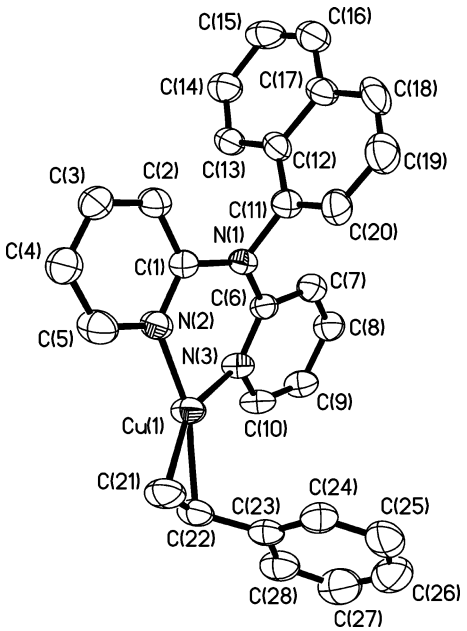

Fig. 18 Structure of the $[Cu(1\text{-naph-dpa})(\eta^2\text{-styrene})]^+$ cation in compound **16**. Thermal ellipsoids are shown at the 30% level, and hydrogen atoms attached to carbon are omitted for clarity.

The PF_6^- anion in **17** also exhibits a site-occupancy disorder for four of the six fluorine atoms (Fig. S20†). The structure of the complex cation, $[Cu(Ar\text{–}dpa)(\eta^2\text{-norbornylene})]^+$, in compound **17** is shown in Fig. 19. Selected bond lengths and angles are compared in Table 7 with those of $[Cu(H\text{-dpa})(\eta^2\text{-norbornylene})]^+$ that we have previously reported.[15]

The copper atoms in compounds **13–17** are each coordinated to two pyridine nitrogen atoms and the appropriate olefin; consistent with three-coordinate Cu(I) cation. The Cu–N distances [1.949(3)–1.973(3) Å] are within experimental error of the analogous ethylene and cyclohexene complexes [1.963(2)–1.973(3) Å].[16,17] In a similar manner the Cu–C distances [1.972(5)–2.064(2) Å]

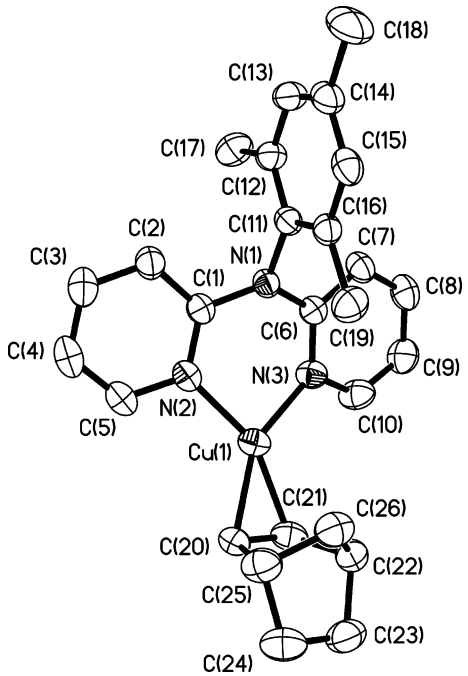

Fig. 19 Structure of the $[Cu(Mes\text{-dpa})(\eta^2\text{-norbornylene})]^+$ cation in compound **17**. Thermal ellipsoids are shown at the 30% level, and hydrogen atoms attached to carbon are omitted for clarity.

overlap the range for the previously reported derivatives [2.019(3)–2.032(4) Å].[15,16,17] The C═C bond determined for compound **17** [1.361(5) Å] is somewhat lengthened compared to free norbornylene [1.334(1) Å],[40] and is slightly shorter than those observed in the neutral iminophosphanamide-norbornylene and diethylenetriamine (detn) complexes [1.37(2) and 1.38(2) Å, respectively],[14,41] as well as the H–dpa complex $[Cu(H\text{–}dpa)(\eta^2\text{-norbornylene})]^+$ [1.388(7) Å].[15]

As we noted above, the presence of *ortho*-substitution in the uncomplexed Ar–dpa compounds results in a significant distortion of the coordination around the amine nitrogen. Additional distortions, resulting in the ligand to fold along the Cu···N vector, occur when the ligand is bound to a copper. In the olefin complexes (**13–16**), both of these deformations are observed. Importantly, however, the folding along the Cu···N vector (*i.e.*, formation of a butterfly conformation) is related to the size of the ligand's aryl group (Fig. 20). This is amply demonstrated by a comparison of the ligand dpa and styrene conformations for the two crystallographically unique conformers of the $[Cu(1\text{-naph-dpa})(\eta^2\text{-styrene})]^+$ cation present in compound **16**, Fig. 21.

The increased folding of the Ar–dpa ligand can be seen from the $[Cu(Ar\text{–}dpa)(\eta^2\text{-styrene})]^+$ cations viewed down the Cu···N vector (Fig. 22). Furthermore, as may be seen from Fig. 22, there is a clear steric consequence of the butterfly conformation of the Ar–dpa ligand on the olefin ligand. Based upon this observation we propose that the complexation of a mono-substituted or *cis*-substituted olefin should be favored over complexation of a *trans*-substituted olefin in complexes where the Ar-dpa ligand has the most distortion due to a sterically large aryl substituent (Ar). Thus, for the *trans*-olefin (**IV**) there will be inter-ligand interactions irrespective of the olefin conformation, while for a *cis*-olefin (**V**) the substituents could adopt a conformation that limits steric

Table 6 Selected bond lengths (Å) and angles (°) for [Cu(Ar–dpa)(η²-styrene)]BF_4

Compound	H–dpa	**13**	**14**[a]	**15**	**16**[a]
R	H	Ph	Mes	(2-^{i}Pr)Ph	naph
Cu(1)–C	1.990(6)	1.984(2)	1.972(5), 1.981(6)	1.992(5)	1.978(4), 1.997(4)
Cu(1)–C′	2.044(5)	2.064(2)	2.042(5), 2.032(6)	2.022(5)	2.021(4), 2.027(4)
Cu(1)–N(2)	1.959(5)	1.965(2)	1.968(4), 1.951(4)	1.958(3)	1.949(3), 1.956(3)
Cu(1)–N(3)	1.967(5)	1.956(2)	1.951(4), 1.965(4)	1.973(3)	1.968(3), 1.959(3)
C–C′	1.387(8)	1.381(3)	1.372(7), 1.381(8)	1.395(6)	1.371(6), 1.393(6)
N–CAr	—	1.462(2)	1.455(5), 1.449(5)	1.461(5)	1.463(5), 1.437(4)
N(2)–Cu(1)–N(3)	96.7(2)	95.20(7)	91.9(2), 92.3(2)	92.3(2)	94.0(1), 95.8(1)
C–Cu(1)–C′	40.2(2)	39.82(9)	39.9(2), 40.2(2)	40.7(2)	40.1(2), 40.5(2)
Cu(1)–C–CPh	108.6(4)	114.9(1)	113.1(4), 109.1(4)	109.8(3)	110.3(3), 108.5(3)

[a] Two crystallographically independent molecules in the asymmetric unit. Atom numbering scheme for the second molecule given in Fig. S15 and S19.†

Table 7 Selected bond lengths (Å) and angles (°) for [Cu(Ar–dpa)(η²-norbornylene)]$^+$

R	H	Mes (**17**)
Cu(1)–C	2.026(6)	2.027(3)
Cu(1)–C′	2.030(6)	2.007(4)
Cu(1)–N(2)	1.957(5)	1.957(3)
Cu(1)–N(3)	1.962(5)	1.961(3)
C–C′	1.388(7)	1.361(5)
N–CAr	—	1.466(4)
Cu···H	2.46	2.46(4)
N(2)–Cu(1)–N(3)	97.7(2)	94.0(1)
C–Cu(1)–C′	40.0(2)	39.5(2)

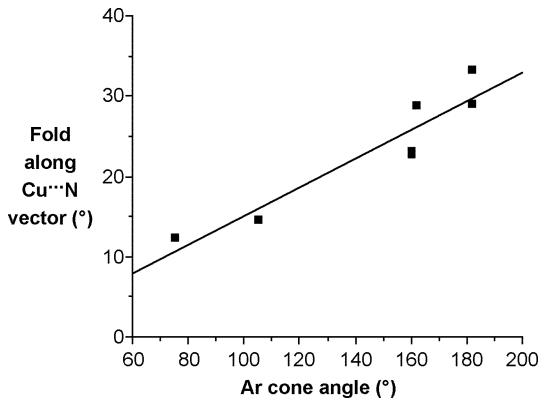

Fig. 20 Plot of the folding of the Ar–dpa ligand as a function of the substituent's cone angle (°) for [Cu(Ar–dpa)(η²-styrene)]$^+$.

interactions. The alternative view of the norbornylene complex cation [Cu(Ar-dpa)(η²-norbornylene)]$^+$ in compound **17** shown in Fig. 23 shows the preferred orientation of a *cis*-substituted olefin with its substituents away from the Ar–dpa ligand. We are currently investigating the selectivity of olefin coordination as a function of the Ar–dpa ligand.

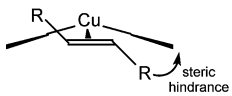

(**IV**)

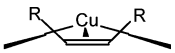

(**V**)

We have previously shown[15] that the bond distances around copper in [Cu(H–dpa)(η²-olefin)]$^+$ do not correlate with changes in binding constant. Instead we have shown that the difference in the ^{1}H and ^{13}C NMR shift values between free and complexed

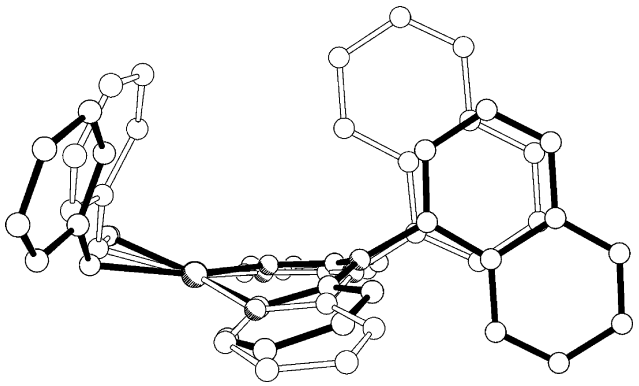

Fig. 21 Comparison of the two crystallographically unique conformers of the [Cu(1-naph-dpa)(η²-styrene)]$^+$ cation present in compound **16**.

olefins can be used to compare binding interactions and compare well with the temperature of dissociation of the olefin in the solid state as determined by TGA. Fig. 24 shows that the change in the ^{1}H and ^{13}C NMR chemical shifts for the styrene ligand in [Cu(Ar–dpa)(η²-styrene)]$^+$ as compared to uncomplexed styrene (*i.e.*, $\Delta\delta$) is indeed related to the stability of the Cu···styrene interaction as determined by the compounds decomposition temperature. Thus, the binding efficiency of an olefin to the copper is affected by the identity of the remote aryl substituent.

In the case of the aryl substituted ligands (*i.e.*, Ar–dpa), the binding efficiency follows the order: Ph ≪ 1-naph < 2-^{i}PrC$_6$H$_4$ < Mes. In fact, the complex stability is directly related to the steric bulk (cone angle) of the aryl, see Fig. 25. However, what is interesting is that the complex of the parent ligand (H–dpa) shows a complex stability almost equal to that of the Mes–dpa complex, despite the difference in steric bulk, and hence folding of the ligand. We conclude that the stability of the Cu···olefin interaction is controlled by both electronic and remote steric effects. A strong Cu···olefin interaction is enabled by either an electron donating substituent at the central nitrogen of the dpa ligand or a sterically large substituent at the central nitrogen of the dpa ligand. The first effect is presumably due to the increased electron density on copper and thence increased π back-donation to the olefin. We propose that the second effect is due to the increased folding of the dpa ligand (Fig. 20), resulting in a decrease in intra-complex inter-ligand steric hindrance, and thus allowing for a tighter binding of the olefin to the copper.

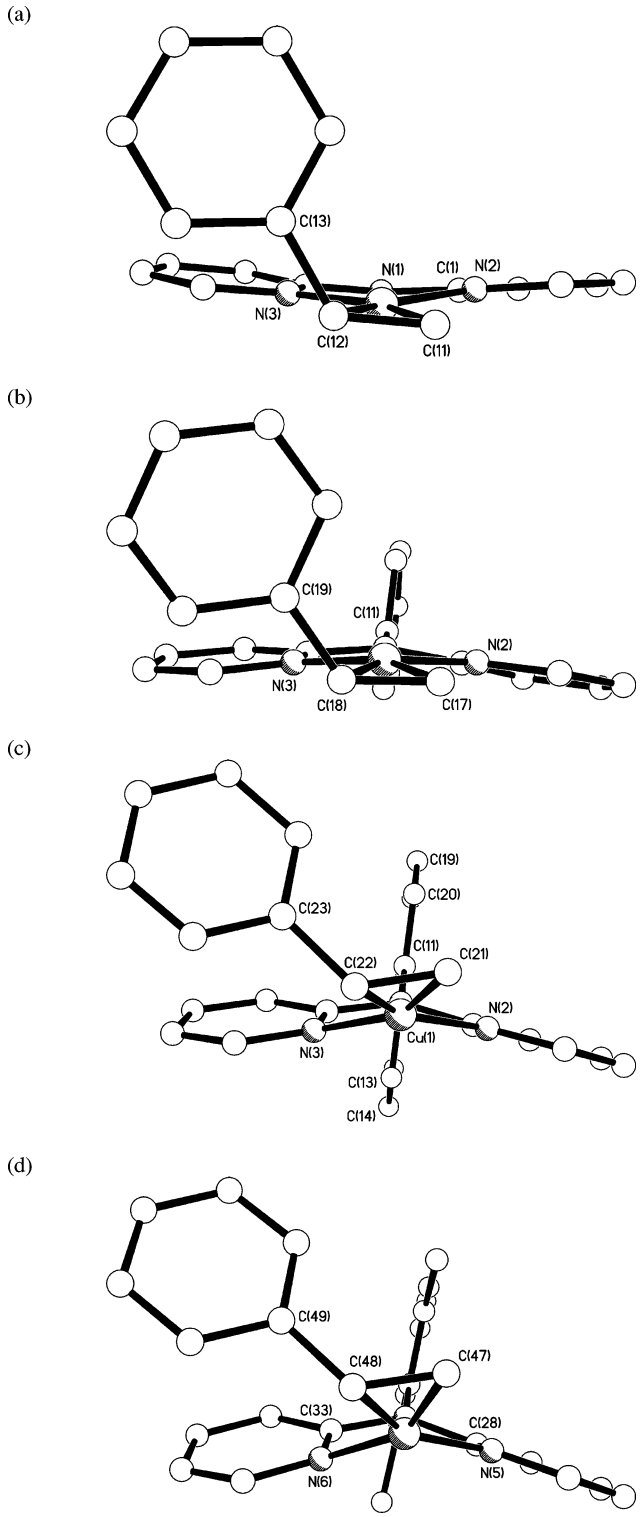

Fig. 22 The folding of the Ar–dpa ligand in the [Cu(Ar–dpa)(η²-styrene)]⁺ cations as viewed along the Cu···N vector, for Ar – H (a), Ph (b), 1-naph (c), and Mes (d).

Conclusions

We have shown that for a range of aryl-substituted *bis*(2-pyridyl)amine ligands the presence of *ortho*-substitution in the uncomplexed Ar–dpa compounds results in a significant distortion

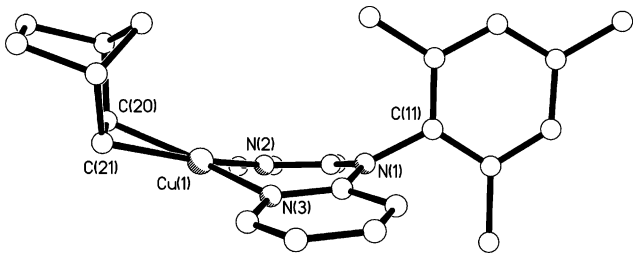

Fig. 23 Alternative view of the [Cu(Mes-dpa)(η²- norbornylene)]⁺ cation showing the preferred orientation of the *cis*-substituted olefin and the Mes-dpa ligand.

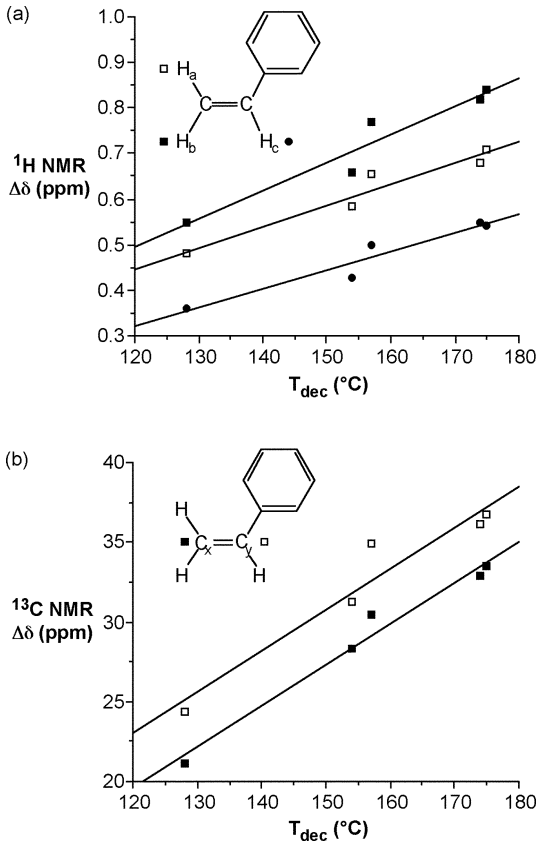

Fig. 24 Plots of the difference in chemical shift (Δδ) for styrene (a) 1H and (b) ^{13}C NMR spectra between free styrene and [Cu(Ar–dpa)(η²-styrene)]BF$_4$ *versus* the temperature for dissociation of the styrene. R_2 values are as follows: (a) □ = 0.922, ■ = 0.897, ● = 0.906 (b) ■ = 0.967, □ = 0.932.

of the coordination around the amine nitrogen (in the solid state) and twisting of the two pyridyl rings with respect to each other. Thus, the steric bulk of the aryl substituents have a controlling influence on the orientation of the pyridyl rings. The presence of *ortho*-substitution in the complexed Ar-dpa compounds, in which the two pyridyl rings are constrained by a complexed atom, results in the bending-up of the aryl ring substituent out of the pyridyl plane with consequential folding of the two pyridyls into a "butterfly" conformation. For olefin complexes of the type [Cu(Ar–dpa)(η²-styrene)]BF$_4$, the increased steric bulk of the aryl group results in the folding of the dpa ligand and the subsequent facial differentiation of the complex so as to favor *cis*- or mono-substituted olefins. In addition, binding interaction of the olefin

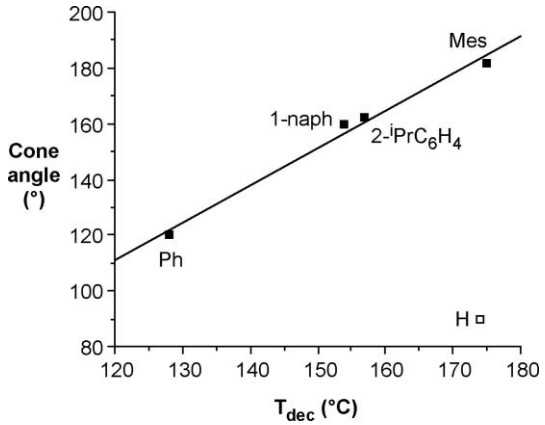

Fig. 25 Plot of relationship between the temperature for dissociation of the styrene in and [Cu(Ar–dpa)(η²-styrene)]BF_4 as a function of the Toleman cone angle (°) of the aryl substituent (R_2 = 0.988). The value for the parent [Cu(Ar–dpa)(η²-styrene)]BF_4 is shown for comparison (□).

with the copper is controlled by the steric bulk of the remote aryl group. We are presently investigating the use of substituted *bis*(2-pyridyl)amine copper complexes for the separation of olefins. These results will be reported elsewhere.

Experimental

All reagents in this study were used as received from commercial suppliers and were stored under an argon atmosphere in a drybox. All solvents were distilled and degassed *via* freeze–pump–thaw immediately prior to use. Glassware was thoroughly cleaned and dried prior to use. All manipulations were performed under an argon atmosphere using standard Schlenk line techniques. Precursor complex [Cu(MeCN)$_4$]BF_4 was prepared according to Hathaway, *et al.*[42] Precursors for the ligands, ArN(H)py (Ar = Ph, 2,4,6-Me_3Ph, 2,6-Et_2Ph, 2,6-$^iPr_2$Ph, and 1-naphthyl), were prepared according to previously reported methods.[20,23] N-phenyl-*N*,*N*-(2,2′-dipyridyl)amine (Ph–dpa) was prepared according to the literature methods.[25] ^{1}H and ^{13}C NMR spectra were obtained at room temperature using Bruker Avance 400 and 500 MHz spectrometers. Chemical shifts are reported relative to internal solvent resonances. IR spectra were obtained using a Nicolet FTIR spectrometer equipped with an ATR accessory. Thermogravimetric analyses were performed on a Seiko I TG/DTA 200 under an argon gas flow of 10–15 mL min^{-1}. GC-MS analyses were performed using Agilent Technologies 5973 network mass selective detector, equipped with 6890 N network GC system.

2-^{i}PrC$_6$H$_4$N(H)(C$_5$H$_4$N) (1)

2-isopropylaniline (49.86 g, 0.369 mol) and 2-bromopyridine (29.13 g, 0.184 mol) were refluxed under an argon atmosphere for 12 h. The reaction mixture was then made alkaline with a saturated solution of Na_2CO_3, followed by steam distillation to remove excess reactants. Extraction with Et_2O, followed by removal of the solvent in vacuum gave an off-white powder. The crude product was recrystallized by the slow evaporation of methanol solution to afford colorless crystals. Yield: 32.24 g (82%). Mp (TGA; sublim.): 120–122 °C. MS (EI, %): *m*/*z* 212 (M^+, 8.7), 169 (M^+ – ^{i}Pr, 100). ^{1}H-NMR ($CDCl_3$): δ 8.14 [1H, ddd, *J*(H–H) = 5.1 Hz, *J*(H–H) = 1.9 Hz,*J*(H–H) = 0.7 Hz, 6-C*H*, py], 7.44 [1H, ddd, *J*(H–H) = 8.5 Hz, *J*(H–H) = 7.2 Hz, *J*(H–H) = 1.9 Hz, 4-C*H*, py], 7.37–7.35 (2H, m, C*H*, Ph), 7.23–7.20 (2H, m, C*H*, Ph), 6.69 [1H, ddd, *J*(H–H) = 7.2 Hz, *J*(H–H) = 5.1 Hz, *J*(H–H) = 0.8 Hz, C*H*, 5-py], 6.67 (1H, br s, N*H*), 6.57 [1H, ddd, *J*(H–H) = 8.5 Hz, *J*(H–H) = 0.8 Hz,*J*(H–H) = 0.7 Hz, C*H*, 3-py], 3.23 [1H, sept, *J*(H–H) = 6.8 Hz, C*H*(CH_3)$_2$], 1.23 [6H, d, *J*(H–H) = 6.8 Hz, CH(C*H*$_3$)$_2$].

Mes–dpa (2)

N-(2,4,6-trimethyl)phenyl-*N*-(2-pyridyl)amine (21.23 g, 100 mmol), sodium *tert*-butoxide (11.53 g, 120 mmol), $Pd_2(dba)_3$ (2.289 g, 2.5 mmol), and DPPF (2.772 g, 5.0 mmol) were added to a Schlenk flask in a drybox. The flask was capped with a septum, removed from the drybox, and toluene (*ca.* 15 mL) was added *via* cannula. The mixture was stirred, and 2-bromopyridine (19.02 g, 120 mmol) was injected *via* syringe into the reaction vessel. The reaction was stirred under nitrogen at 90 °C for 120 h. After cooling, $CHCl_3$ (50 mL) was added, the mixture was filtered, and the solvent was removed under vacuum. The crude product was purified by column chromatography on silica gel (eluent: 5% ethyl acetate in hexanes). The purified product was recrystallized by cooling a saturated solution in hexanes to –12 °C for several days, giving colorless crystals. Yield: 20.58 g (71%). Mp (TGA; sublim.): 141–143 °C. MS (EI,%): *m*/*z* 289 (M^+, 13.2), 274 (M^+ - Me, 100). ^{1}H-NMR (CD_3OD): δ 8.17 [2H, ddd, *J*(H–H) = 5.0 Hz, *J*(H–H) = 1.9 Hz, *J*(H–H) = 0.7 Hz, C*H*, 6,6′-py], 7.65 [2H, ddd, *J*(H–H) = 8.6 Hz, *J*(H–H) = 7.2 Hz, *J*(H–H) = 1.9 Hz, C*H*, 4,4′-py], 7.01 (2H, s, C6*H*2), 6.98 [2H, ddd, *J*(H–H) = 7.2 Hz, *J*(H–H) = 5.0 Hz, *J*(H–H) = 0.9 Hz, C*H*, 5,5′-py], 6.88 [2H, ddd, *J*(H–H) = 8.6 Hz, *J*(H–H) = 0.9 Hz, *J*(H–H) = 0.7 Hz, C*H*, 3,3′-py], 2.33 (3H, s, *p*-C*H*3), 1.96 (6H, s, *o*-C*H*3).

2,6-$Et_2C_6H_3$–dpa (3)

Prepared in an analogous manner to that of compound **2**, using N-(2,6-diethyl)phenyl-*N*-(2-pyridyl)amine (2.26 g, 10 mmol), 2-bromopyridine (1.89 g, 12 mmol), sodium *tert*-butoxide (1.53 g, 16 mmol), $Pd_2(dba)_3$ (137 mg, 0.15 mmol), DPPF (166 mg, 0.30 mmol), and toluene (15 mL). The purified product was recrystallized by cooling a saturated solution in $CHCl_3$ to –12 °C for several days to give colorless crystals. Yield: 0.77 g (25%). Mp (TGA; sublim.): 86–88 °C. MS (EI, %): *m*/*z* 303 (M^+, 2.2), (M^+ – Et, 100). ^{1}H-NMR (298 K; $CDCl_3$): δ 8.28 [2H, ddd, *J*(H–H) = 5.0 Hz, *J*(H–H) = 2.0 Hz, *J*(H–H) = 0.8 Hz, C*H*, C*H*, 6,6′-py], 7.49 [2H, ddd, *J*(H–H) = 8.4 Hz, *J*(H–H) = 7.2 Hz, *J*(H–H) = 2.0 Hz, C*H*, 4,4′-py], 7.34 [1H, dd, *J*(H–H) = 7.7 Hz, *J*(H–H) = 7.7 Hz, p- C*H*, Ph], 7.23 [2H, d, *J*(H–H) = 7.7 Hz, m- C*H*, Ph], 6.94 [2H, ddd, *J*(H–H) = 8.4 Hz, *J*(H–H) = 0.9 Hz, *J*(H–H) = 0.8 Hz, C*H*, 3,3′-py], 6.83 [2H, ddd, *J*(H–H) = 7.2 Hz, *J*(H–H) = 5.0 Hz, *J*(H–H) = 0.9 Hz, C*H*, 5,5′-py], 2.44 [4H, q, *J*(H–H) = 7.6 Hz, CH_2CH_3], 0.96 [6H, t, *J*(H–H) = 7.6 Hz, CH_2CH_3].

2-^{i}PrC$_6$H$_4$–dpa (4)

Prepared in an analogous manner to that of compound **2**, using N-(2-isopropyl)phenyl-*N*-(2-pyridyl)amine (10.645 g, 50 mmol), 2-bromopyridine (9.980 g, 60 mmol), sodium *tert*-butoxide (5.765 g, 60 mmol), $Pd_2(dba)_3$ (1.373 g, 1.25 mmol), DPPF (1.663 g, 2.5 mmol), and toluene (200 mL). The crude product was purified

by column chromatography on silica gel (eluent: 5% ethyl acetate in hexanes). The purified product was recrystallized by a slow evaporation of a 4 : 1 hexanes : CH_2Cl_2 solution to give colorless crystals. Yield 5.311 g (38%). Mp (TGA; sublim.): 101–103 °C. MS (EI,%): *m/z* 289 (M^+, 0.7), 246 (M^+ – ^{i}Pr, 100). ^{1}H-NMR (CD_3OD): δ 8.18 [2H, ddd, J(H–H) = 5.0 Hz, J(H–H) = 2.0 Hz, J(H–H) = 0.8 Hz, C*H*, 6,6′-py], 7.65 [2H, ddd, J(H–H) = 8.4 Hz, J(H–H) = 7.3 Hz, J(H–H) = 2.0 Hz, C*H*, 4,4′-py], 7.47 [1H, dd, J(H–H) = 7.9 Hz, J(H–H) = 1.5 Hz, C*H*, Ph], 7.39 [1H, ddd, J(H–H) = 7.9 Hz, J(H–H) = 7.2 Hz, J(H–H) = 1.3 Hz, C*H*, Ph], 7.29 [1H, ddd, J(H–H) = 7.9 Hz, J(H–H) = 7.2 Hz, J(H–H) = 1.5 Hz, C*H*, Ph], 7.15 [1H, dd, J(H–H) = 7.9 Hz, J(H–H) = 1.3 Hz, C*H*, Ph], 6.99 [2H, ddd, J(H–H) = 7.3 Hz, J(H–H) = 5.0 Hz, J(H–H) = 1.0 Hz, C*H*, 5,5′-py], 6.88 [2H, ddd, J(H–H) = 8.4 Hz, J(H–H) = 1.0 Hz, J(H–H) = 0.8 Hz, C*H*, 3,3′-py], 3.05 [1H, sept, J(H–H) = 6.8 Hz, C*H*(CH_3)$_2$], 0.99 [6H, d, J(H–H) = 6.8 Hz, CH(C*H*$_3$)$_2$].

2,6-^{i}Pr$_2$C$_6$H$_3$–dpa (5)

Prepared in an analogous manner to that of compound **2**, using 2,6-diisopropylaniline (0.355 g, 2.0 mmol), 2-bromopyridine (0.700 g, 4.4 mmol), sodium *tert*-butoxide (0.550 g, 5.7 mmol), $Pd_2(dba)_3$ (0.055 g, 0.06 mmol), DPPF (0.083 g, 0.15 mmol), and toluene (10 mL). The crude product was purified by flash chromatography on silica gel (eluent: 2% MeOH in CH_2Cl_2) followed by recrystallization by vapor diffusion of pentane into a saturated $CHCl_3$ solution yielding colorless crystals Yield: yield 0.331 g (50%). Mp (TGA; sublim.): 95–97 °C. MS (EI, %): *m/z* 331 (M^+, 0.8), 288 (M^+ – ^{i}Pr, 100). ^{1}H-NMR ($CDCl_3$): δ 8.27 [2H, ddd, J(H–H) = 5.0 Hz, J(H–H) = 1.9 Hz, J(H–H) = 0.8 Hz, C*H*, 6,6′-py], 7.50 [2H, ddd, J(H–H) = 8.4 Hz, J(H–H) = 7.2 Hz, J(H–H) = 1.9 Hz, C*H*, 4,4′-py], 7.42 [1H, dd, J(H–H) = 7.7 Hz, J(H–H) = 7.7 Hz, *p*- C*H*, Ph], 7.27 [2H, d, J(H–H) = 7.7 Hz, *m*- C*H*, Ph], 6.96 [2H, ddd, J(H–H) = 8.4 Hz, J(H–H) = 0.9 Hz, J(H–H) = 0.8 Hz, C*H*, 3,3′-py], 6.82 [2H, ddd, J(H–H) = 7.2 Hz, J(H–H) = 5.0 Hz, J(H–H) = 0.9 Hz, C*H*, 5,5′-py], 3.09 [2H, sept, J(H–H) = 6.9 Hz, C*H*(CH_3)$_2$], 0.95 [12H, d, J(H–H) = 6.9 Hz, CH(C*H*$_3$)$_2$].

1-Naph–dpa (6)

Prepared in an analogous manner to that of compound **2**, using N-(1-naphthyl)-*N*-(2-pyridyl)amine (2.20 g, 10 mmol), 2-bromopyridine (1.89 g, 12 mmol), sodium *tert*-butoxide (1.53 g, 16 mmol), $Pd_2(dba)_3$ (137 mg, 0.15 mmol), DPPF (166 mg, 0.30 mmol), and toluene (15 mL). The purified product was recrystallized by a slow evaporation of a 1 : 1 hexanes : CH_2Cl_2 solution to yield 1.37 g (46%) colorless crystals. Mp (TGA; sublim.): 166–168 °C. MS (EI,%): *m/z* 297 (M^+, 41.9), 296 (M^+ – H, 100). ^{1}H-NMR ($CDCl_3$): δ 8.34 [2H, ddd, J(H–H) = 5.0 Hz, J(H–H) = 2.0 Hz, J(H–H) = 0.8 Hz, C*H*, *6,6′*-py], 7.91 [1H, d, J(H–H) = 8.2 Hz, C*H*, naph], 7.88 [1H, d, J(H–H) = 8.2 Hz, C*H*, naph], 7.84 [1H, ddd, J(H–H) = 8.5 Hz, J(H–H) = 1.8 Hz, J(H–H) = 0.9 Hz, C*H*, naph], 7.55 [1H, dd, J(H–H) = 8.2 Hz, J(H–H) = 7.2 Hz, C*H*, naph], 7.49 [2H, ddd, J(H–H) = 8.4 Hz, J(H–H) = 7.3 Hz, J(H–H) = 2.0 Hz, C*H*, 4,4′-py], 7.47 (2H, m, C*H*, naph), 7.37 [1H, ddd, J(H–H) = 8.3 Hz, J(H–H) = 6.9 Hz, J(H–H) = 1.2 Hz, C*H*, naph], 6.90 [2H, ddd, J(H–H) = 8.4 Hz, J(H–H) = 1.0 Hz, J(H–H) = 0.8 Hz, C*H*, 3,3′-py], 6.89 [2H, ddd, J(H–H) = 7.3 Hz, J(H–H) = 5.0 Hz, J(H–H) = 1.0 Hz, C*H*, 5,5′-py].

[(Mes-dpa)H]BF$_4$ (7)

In a 25 mL round bottom flask, compound **2** (0.289 g, 1.0 mmol) was dissolved in MeOH (5 mL). With stirring, KBF_4 (0.130 g, 1.0 mmol) dissolved in dilute HCl (5 mL). The mixture was allowed to stir for 30 min, followed by extraction with CH_2Cl_2 (2 × 5 mL) The solvent was removed under vacuum, and the solid was dissolved in methanol, followed by filtration through a medium porosity sintered-glass frit. Slow evaporation of the filtrate yielded 0.156 g (41%) colorless crystals. Mp (TGA; decomp.): 228–229 °C. ^{1}H-NMR (CD_3OD): δ 8.60 [2H, ddd, J(H–H) = 5.7 Hz, J(H–H) = 1.9 Hz, J(H–H) = 0.7 Hz, C*H*, 6,6′-py], 8.05 [2H, ddd, J(H–H) = 8.9 Hz, J(H–H) = 7.3 Hz, J(H–H) = 1.9 Hz, C*H*, 4,4′-py], 7.42 [2H, ddd, J(H–H) = 7.3 Hz, J(H–H) = 5.7 Hz, J(H–H) = 0.8 Hz, C*H*, 5,5′-py], 7.28 (2H, s, C_6H_2), 6.63 [2H, ddd, J(H–H) = 8.9 Hz, J(H–H) = 0.8 Hz, J(H–H) = 0.7 Hz, C*H*, 3,3′-py], 2.45 (3H, s, *p*-C*H*$_3$), 2.02 (6H, s, *o*-C*H*$_3$).

[(2-^{i}PrC$_6$H$_4$-dpa)H]BF$_4$ (8)

This compound was prepared in an analogous manner to that of compound (**7**), using 0.289 g (1.0 mmol) of compound **4**. Crystals suitable for X-ray diffraction were obtained cooling a saturated solution in ^{i}PrOH to −12 °C for several days. Yield = X g (78%). Mp (TGA; decomp.): 222–224 °C. ^{1}H-NMR (CD_3OD): δ 8.58 [2H, ddd, J(H–H) = 5.7 Hz, J(H–H) = 1.9 Hz,J(H–H) = 0.7 Hz, C*H*, 6,6′-py], 8.02 [2H, ddd, J(H–H) = 8.9 Hz, J(H–H) = 7.3 Hz,J(H–H) = 1.9 Hz, C*H*, 4,4′-py], 7.78 (1H, C*H*), 7.75 (1H, C*H*), 7.60 (1H, C*H*),7.45 (1H, C*H*), 7.41 [2H, ddd, J(H–H) = 7.3 Hz, J(H–H) = 5.7 Hz,J(H–H) = 0.8 Hz, C*H*, 5,5′-py], 6.65 [2H, ddd, J(H–H) = 8.9 Hz, J(H–H) = 0.8 Hz,J(H–H) = 0.7 Hz, C*H*, 3,3′-py], 2.80 [1H, sept, J(H–H) = 8.9 Hz, C*H*(CH_3)$_2$], 1.08 [6H, d, J(H–H) = 8.9 Hz, CH(C*H*$_3$)$_2$].

[Cu(Ph-dpa)(Cl)(μ-Cl)]$_2$ (9)

[Cu(MeCN)$_4$]BF_4 (0.157 g, 0.5 mmol) and Ph-dpa (0.124 g, 0.5 mmol) were stirred together in tetraethylene glycol (2 mL) in a conical vial open to the atmosphere, until all solids had dissolved. Dilute HCl (2 mL) was then added to the mixture, turning the dark blue/green solution milky white. The mixture was then extracted with CH_2Cl_2 (2 × 5 mL), and the combined organic layers were allowed to evaporate. The resulting brown residue was taken up in MeOH (5 mL), which was filtered and cooled to −12 °C for several days, yielding dark green plates. Yield: 0.114 g (60%). Mp (TGA; decomp.) 265–267 °C.

[Cu(2-^{i}PrC$_6$H$_4$-dpa)(Cl)(μ-Cl)]$_2$ (10)

This compound was prepared in an analogous manner to that of compound **9**, using compound **4** (0.149 g, 0.5 mmol) for the ligand. Recrystallization by slow evaporation of MeOH solution. Yield: 48%. Mp (TGA; decomp.) 231–233 °C.

[Cu(1-naph-dpa)(Cl)(μ-Cl)]$_2$ (11)

This compound was prepared in an analogous manner to that of compound **9**, using compound **6** (0.149 g, 0.5 mmol) for the ligand. Recrystallized by a slow evaporation of MeOH solution. Yield: 48%. Mp (TGA; decomp.) 230–232 °C.

[Cu(Mes–dpa)(H_2O)(μ-OH)]$_2$[BF_4]$_2$ (12)

[Cu(MeCN)4]BF_4 (0.314 g, 1.0 mmol) and **2** (0.289 g, 1.0 mmol) were stirred together in MeOH (5 mL) and H_2O (1 mL) in a vial open to the atmosphere. After the solution had taken on a dark blue color (*ca*. 1 h), the solvent was removed under vacuum, and the resulting powder was dissolved in 5 : 1 MeOH : acetone, filtered, and cooled to −12 °C for several days, yielding dark blue crystals of the methanol solvate. Yield: 0.569 g (56%). Mp (TGA; decomp.) 198–202 °C.

[Cu(Ph–dpa)(η^2-styrene)]BF_4 (13)

In a drybox, [Cu(MeCN)$_4$]BF_4 (0.314 g, 1.0 mmol) and Ph–dpa (0.247 g, 1.0 mmol) were charged to separate Schlenk flasks. After removal from the drybox, EtOH (15 mL) was added *via* cannula to the flask containing the ligand, which was stirred to dissolve the solid. Styrene (*ca*. 3 mL) in EtOH (12 mL) was added *via* cannula to the flask containing the copper precursor. After stirring for one hour, the ligand solution was added to the copper–olefin mixture, and the combined solutions were stirred under an argon atmosphere for 6 h. The solution volume was then reduced under vacuum by approximately half, warmed gently with a water bath to redissolve the product, and then filtered through a medium porosity glass frit to remove insoluble impurities. Argon was vigorously bubbled through the resulting pale green solution to further reduce its volume to *ca.* 5–10 mL. The solution was gently warmed to dissolve any precipitate, and upon cooling to −12 °C for several days, yielded colorless crystals of the ethanol solvate. Yield: 0.203 g (37%). Mp (TGA; decomp.) 128 °C. ^{1}H-NMR (298 K; CD_3OD): δ 8.06 (2H, br s, C*H*, *6*,*6*′-py), 7.83 (2H, br t, C*H*, *4*,*4*′-py), 7.51 (2H, br t, *m*-C*H*, Ph), 7.46 (1H, br s, *p*-C*H*, Ph), 7.43 (2H, mult., *o*-C*H*, styrene), 7.26 (2H, mult., *m*-C*H*, styrene), 7.22 (2H, br s, C*H*, Ph), 7.19 (1H, mult., *p*-C*H*, styrene), 7.17 (2H, br t, C*H*, *5*,*5*′-py), 6.93 (2H, br d, C*H*, *3*,*3*′-py), 6.29 [1H, dd, J(H–H) = 16.4 Hz, J(H–H) = 10.0 Hz, C*H*Ph], 5.13 [1H, d, J(H–H) = 16.4 Hz, *cis*-C*H*, Ph], 4.67 [1H, d, J(H–H) = 10.0 Hz, *trans*-C*H*, Ph], 3.60 [2H, q, J(H–H) = 6.9 Hz, OCH_2CH_3], 1.17 [3H, t, J(H–H) = 6.9 Hz, OCH_2CH_3].

[Cu(Mes-dpa)(η^2-styrene)]BF_4 (14)

This compound was prepared in an analogous manner to that of compound **13**, using 2-butanol as solvent and compound **2** as ligand. Yield: 61%. Mp (TGA; decomp.) 174 °C. ^{1}H-NMR (298 K; CD_3OD): δ 8.33 (2H, br d, C*H*, *6*,*6*′-py), 7.73 [2H, ddd, J(H–H) = 8.9 Hz, J(H–H) = 7.3 Hz, J(H–H) = 2.0 Hz, *m*-sty], 7.46 (2H, m, C*H*, *4*,*4*′-py), 7.24-7.18 (3H, m, C*H*, *3*,*3*′-py and *p*- C*H*, styrene), 7.18 (2H, s, *m*-C*H*, Mes), 7.13 [2H, ddd, J(H–H) = 6.3 Hz, J(H–H) = 5.5 Hz, J(H–H) = 0.9 Hz, C*H*, *5*,*5*′-py], 6.45 [2H, d, J(H–H) = 8.9 Hz, C*H*, *o*-C*H*, styrene], 6.11 [1H, dd, J(H–H) = 15.8 Hz, J(H–H) = 9.6 Hz, C*H*Ph], 4.84 [1H, d, J(H–H) = 15.8 Hz, *cis*-C*H*, styrene], 4.44 [1H, d, J(H–H) = 9.6 Hz, *trans*-C*H*, styrene], 2.38 (3H, s, *p*-CH_3), 1.89 (6H, s, *o*-CH_3).

[Cu(2-^{i}PrC_6H_4-dpa)(η^2-styrene)]BF_4 (15)

This compound was prepared in an analogous manner to that of compound (**13**), using ^{i}PrOH as solvent and compound **4** as ligand. Yield: 66%. Mp (TGA; decomp.) 156–158 °C. ^{1}H-NMR (298 K; CD_3OD): δ 8.31 (2H, br d, C*H*, *6*,*6*′-py), 7.73 (2H, br t, C*H*, *4*,*4*′-py), 7.62 (1H, br d, C*H*, Ph), 7.61 (1H, br t, C*H*, Ph), 7.52 (1H, br t, C*H*, Ph), 7.48 (2H, mult., C*H*, sty), 7.44 (1H, br d, C*H*, Ph), 7.27 (2H, mult., C*H*, sty), 7.23 (1H, mult., *p*-C*H*, sty), 7.14 (2H, br t, C*H*, *5*,*5*′-py), 6.67 (2H, br d, C*H*, *3*,*3*′-py), 6.15 [1H, dd, J(H–H) = 15.7 Hz, J(H–H) = 9.6 Hz, C*H*Ph], 4.90 [1H, d, J(H–H) = 15.7 Hz, *cis*-C*H*, styrene], 4.49 [1H, d, J(H–H) = 9.6 Hz, *trans*-C*H*, styrene], 2.71 [1H, sept, J(H–H) = 6.8 Hz, C*H*$(CH_3)_2$], 0.87 [6H, d, J(H–H) = 6.8 Hz, CH(C*H*$_3)_2$].

[Cu(1-naph-dpa)(η^2-styrene)]BF_4 (16)

This compound was prepared in an analogous manner to that of compound (**13**), using ^{i}PrOH as solvent and compound **6** as ligand. Yield: 58%. Mp (TGA; decomp.) 153–155 °C. ^{1}H-NMR (298 K; CD_3OD): δ 8.24 (2H, br s, *6*-C*H*, py), 8.14 (1H, br d, C–*H*, naph), 8.07 (1H, br d, C–*H*, naph), 7.70 (1H, br t, C–*H*, naph), 7.63 (2H, br t, *4*-C*H*, py), 7.61 (1H, br d, C–*H*, naph), 7.60 (1H, br d, C–*H*, naph), 7.58 (1H, br s, C–*H*, naph), 7.52 (2H, m, C–*H*, sty), 7.48 (1H, br t, C–*H*, naph), 7.30 (2H, m, C–*H*, sty), 7.24 (1H, m, C–*H*, sty),7.12 (2H, br t, *5*-C*H*, py), 6.58 (2H, br d, *3*-C*H*, py), 6.23 [1H, dd, J(H–H) = 15.9 Hz, J(H–H) = 9.8 Hz, C*H*Ph], 5.03 [1H, d, J(H–H) = 15.9 Hz, *cis*-C*H*, styrene], 4.57 [1H, d, J(H–H) = 9.8 Hz, *trans*-C*H*, styrene]

[Cu(Mes-dpa)(η^2-norbornylene)]PF_6 (17)

This compound was prepared in an analogous manner to that of **13**, using 2-butanol as solvent, compound **2** as ligand, and norbornylene as olefin Yield: 76%. Mp (TGA; decomp.) 176–178 °C. ^{1}H-NMR (298 K; CD_3OD): δ 8.56 (2H, br d, *6*-C*H*, py), 7.82 (2H, br t, *4*-C*H*, py), 7.25 (2H, br t, *5*-C*H*, py), 7.23 (2H, s, C*H*), 6.52 (2H, br d, *3*-C*H*, py), 5.10 (2H, br s, *H*C=C*H*), 3.13 (2H, br s, C*H*CH_2C*H*), 2.42 (3H, s, *p*-CH_3), 1.97 (6H, s, *o*-CH_3), 1.66 (2H, m, CH_2), 1.29 (1H, m, CHCH_2CH), 1.12 (2H, m, CH_2), 0.99 (1H, m, CHCH_2CH).

[Cu(2-^{i}PrC_6H_4-dpa)(η^2-norbornylene)]BF_4 (18)

This compound was prepared in an analogous manner to that of compound **17**, using ^{i}PrOH as solvent and compound **4** as ligand. Yield: 66%. Mp (TGA; decomp.) 152–155 °C. ^{1}H-NMR (298 K; CD_3OD): δ 8.54, 7.80, 7.69 (1H, br d, C*H*, Ph), 7.66 (1H, br t, C*H*, Ph), 7.56 (1H, br t, C*H*, Ph), 7.45 (1H, br d, C*H*, Ph), 7.25 (2H, br t, C*H*, 5-Py), 6.68 (2H, br d, C*H*, 3-Py), 5.11 (2H, br s, *H*C=C*H*), 3.12 (2H, br s, C*H*CH_2C*H*), 2.87 [1H, sept, J(H–H) = 7.0 Hz, C*H*$(CH_3)_2$], 1.67 (2H, m, CH_2), 1.30 (1H, m, CHCH_2CH), 1.12 (2H, m, C*H*2), 1.01 (1H, m, CHCH_2CH), 0.97 [6H, d, J(H–H) = 7.0 Hz, CH(C$H_3)_2$].

Crystallographic studies

X-ray data for compounds **1–17** were collected at room temperature (with the exception of **13**, for which data was collected at 213 K) on a Bruker SMART 1000 CCD diffractometer equipped with graphite monochromated Mo-Kα radiation (λ = 0.71073 Å) and corrected for Lorentz and polarization effects. Samples were prepared for single crystal X-ray diffraction by suspending crystal samples in mineral oil under an inert atmosphere, followed by sealing in a thin layer of epoxy resin and securing to the end of a

Table 8 Summary of X-ray diffraction data

Compound	**1**	**2**	**3**	**4**	**5**	**6**	**7**	**8**
Empir. formula	$C_{14}H_{16}N_2$	$C_{19}H_{19}N_3$	$C_{20}H_{21}N_3$	$C_{19}H_{19}N_3$	$C_{22}H_{25}N_3$	$C_{20}H_{15}N_3$	$C_{19}H_{20}N_3BF_4$	$C_{19}H_{20}N_3BF_4$
M_W	212.29	289.37	303.40	289.37	331.45	297.35	377.19	377.19
Cryst. system	Monoclinic	Orthorhombic	Monoclinic	Orthorhombic	Triclinic	Monoclinic	Monoclinic	Monoclinic
Space group	$P2_1/n$	$P2_12_12_1$	$P2_1$	$Pna2_1$	$P\bar{1}$	$P2_1/c$	$P2_1/c$	$P2_1/n$
a/Å	10.327(2)	7.264(1)	8.546(1)	14.616(3)	8.366(1)	7.825(1)	8.730(1)	8.841(1)
b/Å	10.601(2)	13.053(3)	17.299(4)	8.891(1)	14.390(3)	11.121(2)	10.151(2)	19.190(4)
c/Å	12.450(3)	17.072(3)	11.402(2)	24.367(5)	16.817(3)	17.574(4)	21.326(4)	11.776(2)
α (°)	—	—	—	—	100.90(3)	—	—	—
β (°)	112.81(3)	—	92.17(3)	—	100.91(3)	92.04(3)	93.43(3)	94.00(3)
γ (°)	—	—	—	—	95.05(3)	—	—	—
V/Å^3	1256.5(5)	1618.7(6)	1684.4(6)	3166(1)	1935.8(7)	1528.4(5)	1886.5(6)	1993.0(7)
Z	4	4	4	8	4	4	4	4
D_c/g cm^{-3}	1.122	1.187	1.196	1.214	1.137	1.292	1.328	1.257
μ/mm^{-1}	0.067	0.071	0.072	0.073	0.068	0.078	0.107	0.101
2θ range (°)	4.38–56.58	3.92–56.82	3.58–56.62	3.34–56.60	2.52–57.00	4.34–56.62	3.82–56.70	4.06–58.30
No. collected	15089	19614	20430	37351	22485	17948	22802	24786
No. ind. (R_{int})	3042 (0.0369)	2274 (0.0694)	4213 (0.0705)	3996 (0.0626)	9008 (0.0897)	3704 (0.0416)	4646 (0.0615)	5040 (0.0876)
No. obsd. ($\|F_o\| > 4.0\sigma \|F_o\|$)	1876	1323	1901	2240	2967	2206	1996	1540
R	0.0480	0.0444	0.0491	0.0517	0.0608	0.0417	0.059	0.0645
R_w	0.1180	0.1112	0.11181	0.1225	0.1460	0.0984	0.1503	0.1694
Largest difference peak and hole/e Å^{-3}	0.134, –0.151	0.136, –0.141	0.246, –0.159	0.319, –0.198	0.267, –0.288	0.136, –0.139	0.352, –0.183	0.189, –0.196
Weights	0.0615, 0.2646	0.0703, 0.0731	0.0827, 0	0.0868, 0.2396	0.0942, 0	0.0521, 0.2599	0.0815, 0.1418	0.0932, 0
CCDC Deposit No.	720342	720335	720338	720339	720340	720337	720347	735399

Table 8 *(Contd.)*

Compound	9	10	11	12	13	14	15	16	17
Empir. formula	$Cu_2C_{32}H_{26}N_6Cl_4$	$Cu_2C_{38}H_{38}N_6Cl_4$	$Cu_2C_{42}H_{38}N_6Cl_4O_2$	$Cu_2C_{40}H_{52}N_6O_6B_2F_8$	$CuC_{26}H_{27}N_3OBF_4$	$CuC_{27}H_{27}N_3BF_4$	$CuC_{27}H_{27}N_3BF_4$	$CuC_{28}H_{23}N_3BF_4$	$CuC_{27}H_{33}N_3PF_6O$
M_W	763.47	847.62	927.66	1013.58	547.86	543.87	543.87	551.84	624.07
Cryst. system	Monoclinic	Orthorhombic	Monoclinic	Monoclinic	Monoclinic	Monoclinic	Monoclinic	Monoclinic	Monoclinic
Space group	$C2/c$	$Pna2_1$	$P2_1/n$	$P2_1/n$	$P2_1/c$	$P2_1/n$	$P2_1/c$	$P2_1/c$	$P2_1/c$
a/Å	16.282(3)	15.295(3)	8.996(1)	12.762(3)	13.238(3)	13.001(3)	14.174(3)	25.745(5)	10.770(2)
b/Å	7.367(1)	9.059(1)	8.060(1)	7.775(1)	11.178(2)	17.616(4)	14.040(3)	13.345(3)	14.380(3)
c/Å	27.085(5)	26.601(5)	28.486(6)	23.501(5)	17.418(4)	23.608(5)	14.366(3)	15.876(3)	18.831(4)
α (°)	—	—	—	—	—	—	—	—	
β (°)	101.28(3)	—	98.00(3)	100.72(3)	103.54(3)	105.69(3)	110.07(3)	102.30(3)	102.61(3)
γ (°)	—	—	—	—	—	—	—	—	
V/Å^3	3186(1)	3686(1)	2045.7(7)	2291.4(8)	2505.7(9)	5205(1)	2685(1)	5329(1)	2846(1)
Z	4	4	2	2	4	8	4	8	4
D_c/g cm^{-3}	1.592	1.527	1.506	1.469	1.452	1.388	1.345	1.376	1.456
μ/mm^{-1}	1.704	1.481	1.345	1.012	0.926	0.888	0.861	0.869	0.888
2θ range (°)	3.06–56.60	3.06–56.62	2.88–56.72	3.52–56.62	3.16–58.00	2.92–56.62	3.06–55.72	3.24–55.54	3.60–56.72
No. collected	19084	43741	24044	27141	30328	63241	32100	65597	34349
No. ind.	3900	9011	4985	5577	6246	12690	6303	12485	6948
(R_{int})	(0.0331)	(0.0924)	(0.0591)	(0.0686)	(0.0495)	(0.1166)	(0.1004)	(0.0792)	(0.0452)
No. obsd. ($\|F_o\| > 4.0\sigma \|F_o\|$)	3135	5711	3528	3355	4852	4306	2391	5082	3747
R	0.0286	0.0476	0.0870	0.052	0.0411	0.0616	0.0609	0.0602	0.0496
R_w	0.0695	0.1002	0.2496	0.1118	0.1133	0.1381	0.1407	0.1657	0.1305
Largest difference peak and hole/e Å^{-3}	0.285, –0.439	0.481, –0.450	1.697, –0.553	0.690, –0.569	0.497, –0.752	0.358, –0.269	0.298, –0.207	0.590, –0.378	0.384, –0.391
Weights	0.0356, 2.4183	0.0515, 0	0.0886, 13.2506	0.0557, 2.1475	0.0672, 0.9725	0.0975, 0	0.0764, 0	0.0956, 0	0.0776, 1.4546
CCDC Deposit No.	720344	733833	720343	720346	724010	724009	740151	743482	728875

glass fiber. Fibers were fastened onto brass pins and mounted onto a fixed-χ 4-axis goniometer head. Data collection and unit cell refinement were carried out according to established methods[43] using the program SMART.[44] The program SAINT[45] was used for data reduction, and absorption correction was applied using SADABS.[46] Pertinent details are given in Table 8. Heavy atom sites were located by Patterson methods for complex **11**; all other structures were solved by direct methods, and models were refined using full-matrix least squares techniques.[47] Refinement was performed with anisotropic thermal parameters for all non-hydrogen atoms: shift/error less than 0.01. All hydrogen atoms, with the exceptions of those noted below in **1**, **7**, **8**, **12**, and **17**, were placed in calculated positions [C–H (alkyl) = 0.97 Å, C–H (methyl) = 0.96 Å, C–H (aromatic) = 0.93 Å, N–H = 0.86 Å, and O–H = 0.82 Å] and refined with fixed isotropic displacement parameters. The amine hydrogen atom in **1**, the pyridyl-bound hydrogen atoms in **7** and **8**, oxygen-bound H atoms in **12**, and the norbornyl-H atom showing slight interaction with the copper center in **17** were located in the difference map and refined freely. Neutral-atom scattering factors were taken from the usual source.[48] Refinement of positional and anisotropic displacement parameters led to convergence for all data. The program used for structure solution and refinement was SHELXTL Version 6.14.[49] The program PLATON was employed for structure validation, and its squeeze function was utilized for refinement in compounds **8**, **15**, and **16**, which were found to contain solvent accessible voids.[50,51] Selected bond lengths and angles are given in Tables 1–7. Refinement of noncentrosymmetric structures **2** ($P2_12_12_1$), **3** ($P2_1$), **4** ($Pna2_1$), and **10** ($Pna2_1$) was performed according to previously established methods,[52,53] using TWIN/BASF instructions, and merging Friedel pairs for compounds **2–4**.

Compounds **3–5**, **14**, and **16** were found to crystallize with two unique molecules in the asymmetric unit. Structure solution and refinement for compound **3** was performed in the asymmetric space group monoclinic $P2_1$, with TWIN/BASF instructions. Friedel pairs were merged (MERG 4) for refinement. Molecule 2 of the asymmetric unit is shown in Fig. S1,† and a comparison of the two comformers are shown in Fig. S2.† Compound **4** crystallized with 2 unique molecules in the asymmetric unit, one of which exhibited a site occupancy disorder of the isopropyl methyl groups (see ESI for details†). The disorder in molecule 2 of the asymmetric unit is shown in Fig. S3,† and a comparison of the two comformers are shown in Fig. S4.† Molecule 2 of the asymmetric unit of compound **5** is shown in Fig. S5,† and a comparison of the two comformers are shown in Fig. S6.† The numbering schemes for the second unique conformers of complexes **14** and **16** are given in Fig. S15 and S19,† and comparisons of the respective conformers are shown in Figures Fig. S16† and Fig. 21. Refer to ESI† for details concerning disordered anions in **7**, **8**, **12–15**, and **17**.

Acknowledgements

Financial support for this work is provided by Trans Ionics Corporation. The Robert A. Welch Foundation is acknowledged for funding of the Texas Center for Crystallography at Rice University.

References

1 National Research Council, "Separation and Purification: Critical Needs and Opportunities" (National Academy Press, Washington, DC, 1987).
2 J. L. Humphrey, A. F. Seibert and R. A. Koort; Separation Technologies: Advances and Priorities, *DOE(ID(12920-1*, Washington, DC 1001.
3 E. R. Brown and R. L. Hair, Monoolefin(paraffin separation by selective adsorption. Phillips Petroleum Company, 1993.
4 K. Wang and E. I. Stiefel, *Science*, 2001, **291**, 106.
5 J. S. Thompson, R. L. Harlow and J. F. Whitney, *J. Am. Chem. Soc.*, 1983, **105**, 3522.
6 F. I. Rodriguez, J. J. Esch, A. E. Hall, B. M. Binder, G. E. Schaller and A. B. Bleeker, *Science*, 1999, **283**, 996; G. E. Schaller and A. B. Bleeker, *Science*, 1995, **270**, 1809–1811; J. R. Ecker, *Science*, 1995, **268**, 667.
7 W. A. Braunecker, T. Pintauer, N. V. Tsarevsky, G. Kickelbick and K. Matyjaszewski, *J. Organomet. Chem.*, 2005, **690**, 916.
8 X. Dai and T. H. Warren, *Chem. Comm.*, 2001, 1998.
9 B. F. Straub, F. Eisentrager and P. Hofmann, *Chem. Commun.*, 1999, 2507.
10 A. Boni, G. Pampaloni, R. Peloso, D. Belleti, C. Graiff and A. Tiripicchio, *J. Organomet. Chem.*, 2006, **691**, 5602.
11 J. S. Thompson and J. F. Whitney, *Inorg. Chem.*, 1984, **23**, 2813.
12 J. S. Thompson, J. C. Calabrese and J. F. Whitney, *Acta Crystallogr., Sect. C: Cryst. Struct. Commun.*, 1985, **C41**, 890.
13 J. Zhang, R.-G. Xiong, J.-L. Zuo and X.-Z. You, *Chem. Commun.*, 2000, 1495; J. Zhang, R.-G. Xiong, J.-L. Zuo, C.-M. Che and X.-Z. You, *J. Chem. Soc., Dalton Trans.*, 2000, 2898.
14 M. Munakata, S. Kitagawa, S. Kosome and A. Asahara, *Inorg. Chem.*, 1986, **25**, 2622.
15 J. J. Allen and A. R. Barron, *Dalton Trans.*, 2009, 878.
16 J. J. Allen, C. E. Hamilton and A. R. Barron, *J. Chem. Crystallogr.*, 2010, **40**(2), 130.
17 J. J. Allen, C. E. Hamilton and A. R. Barron, *J. Chem. Crystallogr.*, 2010, **40**(2), 137.
18 J. J. Allen, C. E. Hamilton and A. R. Barron, *J. Chem. Crystallogr.*, 2009, **39**(8), 573.
19 M. Polamo and M. Hamalainen, *Z. Kristallogr.–New Cryst. Struct.*, 2002, **217**, 563.
20 M. Polamo, M. Talja and A. J. Piironen, *Z. Kristallogr.–New Cryst. Struct.*, 2005, **220**, 41.
21 M. Polamo and M. Talja, *Z. Kristallogr.–New Cryst. Struct.*, 2004, **219**, 67.
22 M. Polamo and M. Talja, *Z. Kristallogr.–New Cryst. Struct.*, 2004, **219**, 69.
23 M. Polamo, T. Repo and M. Leskela, *Acta Chem. Scand.*, 1997, **51**, 325.
24 H. Schodel, C. Nather, H. Bock and F. Butenschon, *Acta Crystallogr., Sect. B: Struct. Sci.*, 1996, **B52**, 842.
25 J.-S. Yang, Y.-D. Lin, Y.-H. Lin and F.-L. Liao, *J. Org. Chem.*, 2004, **69**, 3517.
26 C. Sumby and P. Steel, *Inorg. Chim. Acta*, 2007, **360**, 2100.
27 I. N. Polyakova, Z. A. Starikova, B. V. Parusnikov and I. A. Krasavin, *Kristallografiya*, 1985, **30**, 1010.
28 I. N. Polyakova, Z. A. Starikova, V. K. Trunov, B. V. Parusnikov and I. A. Krasavin, *Kristallografiya*, 1980, **25**, 495.
29 P. C. Junk, W. Lu, L. I. Semenova, B. W. Skelton and A. H. White, *Z. Anorg. Allg. Chem.*, 2006, **632**, 1303.
30 F. A. Cotton, L. M. Daniels, G. T. Jordan and C. A. Murillo, *Polyhedron*, 1998, **17**, 589.
31 E. Spodine, J. Manzur, M. T. Garland, J. P. Fackler, R. J. Staples and B. Trzcinska-Bancroft, *Inorg. Chim. Acta*, 1993, **203**, 73.
32 B. Viossat, J. F. Gaucher, A. Mazurier, M. Selkti and A. Tomas, *Z. Kristallogr.–New Cryst. Struct.*, 1998, **213**, 329.
33 G. E. Kostakis, E. Norlander, M. Haukka and J. C. Plakatouras, *Acta Crystallogr., Sect. E: Struct. Rep. Online*, 2006, **E62**, m77.
34 L. Lu, S. Qin, P. Yang and M. Zhu, *Acta Crystallogr., Sect. E: Struct. Rep. Online*, 2004, **E60**, m950.
35 X. Dai and T. H. Warren, *Chem. Commun.*, 2001, 1998.
36 J. M. Seco, U. Amador and M. J. Gonzalez Garmendia, *Polyhedron*, 1999, **18**, 3605–3610.
37 D. Petrovic, L. M. R. Hill, P. G. Jones, W. B. Tolman and M. Tamm, *Dalton Trans.*, 2008, 887.
38 M.-M. Yu, Y.-N. Zhang and L.-H. Wei, *Acta Crystallogr., Sect. E: Struct. Rep. Online*, 2007, **E63**, m2380.

39 S. Youngme, J. Phatchimkun, U. Suksangpanya, C. Pakawatchai, G. A. van Albada, M. Quesada and J. Reedijk, *Inorg. Chem. Commun.*, 2006, **9**, 242.
40 J. Min, J. Benet-Buchholz and R. Boese, *Chem. Commun.*, 1998, 2751.
41 M. Pasquali, C. Floriani, A. Gaetani-Manfredotti and A. Chiesi-Villa, *J. Am. Chem. Soc.*, 1978, **100**, 4918.
42 B. J. Hathaway, D. J. Holah and J. D. Postlethwaite, *J. Chem. Soc.*, 1961, 3215.
43 S. Ruhl and M. *Z.* Bolte, *Z. Kristallogr.*, 2000, **215**, 499.
44 *Bruker (2003). SMART v5.63.* Bruker AXS Inc., Madison, WI.
45 *Bruker (2003). SAINT v6.45.* Bruker AXS Inc., Madison, WI.
46 G. M. Sheldrick, (2008) *SADABS*.University of Göttingen, Germany, based on method described in: R. H. Blessing, *Acta Crystallogr.*, 1995, A51, 33.
47 G. M. Sheldrick, *Acta Crystallogr., Sect. A: Found. Crystallogr.*, 2008, **A64**, 112–122.
48 F. H. Allen, O. Kennard, D. G. Watson, L. Brammer, A. G. Orpen and R. Taylor, *International Tables for Crystallography*, Volume C, Ed. A. J. C. Wilson, Dordrecht, Kluwer (1995).
49 G. M. Sheldrick, *SHELXTL v6.14*; *The Complete Software Package for Single Crystal Structure Determination.* Bruker AXS Inc., Madison, WI, 2000.
50 A. L. Spek, *PLATON, A multipurpose Crystallographic Tool.* Utrecht University, Ulrecht. 2000.
51 A. L. Spek, *J. Appl. Crystallogr.*, 2003, **36**, 7.
52 H. D. Flack and G. J. Bernardinelli, *J. Appl. Crystallogr.*, 2000, **33**, 1143.
53 W. Clegg, *Acta Crystallogr., Sect. E: Struct. Rep. Online*, 2003, **E59**, e2.

